



1 Cellulose in atmospheric particulate matter

2

3 Adam Brighty¹, Véronique Jacob¹, Gaëlle Uzu¹, Lucille Borlaza¹, Sébastien Conil²,
4 Christoph Hueglin³, Stuart K. Grange³, Olivier Favez^{4,5}, Cécile Trébuchon⁶, and Jean-Luc
5 Jaffrezo¹

6

7

8

9 ¹University Grenoble Alpes, CNRS, IRD, INP-G, IGE (UMR 5001), 38000 Grenoble, France

10 ²ANDRA, DRD/GES Observatoire Pérenne de l'Environnement, 55290 Bure, France

11 ³Empa, Swiss Federal Laboratories for Materials Science and Technology, Überlandstrasse 129, 8600
12 Dübendorf, Switzerland

13 ⁴Institut national de l'environnement industriel et des risques (INERIS), Parc Technologique Alata
14 BP2, 60550 Verneuil-en-Halatte, France

15 ⁵Laboratoire Central de Surveillance de la Qualité de l'Air (LCSQA), 60550 Verneuil-en-Halatte,
16 France

17 ⁶Atmo AURA, F-38400 Grenoble, France

18

19 **Correspondance:** Adam Brighty (adam.brighty1@gmail.com) and Jean-Luc Jaffrezo (Jean-
20 luc.Jaffrezo@univ-grenoble-alpes.fr)

21

22 **Abstract**

23 The spatiotemporal variations of free cellulose concentrations in atmospheric particles, as a
24 proxy for plant debris, were investigated using a novel HPLC-PAD method. Filter samples
25 were taken from nine sites of varying characteristics across France and Switzerland, with
26 sampling covering all seasons. Concentrations of cellulose, as well as carbonaceous aerosol
27 and other source-specific chemical tracers (e.g. Elemental Carbon (EC), levoglucosan, polyols,
28 trace metals, and glucose) were quantified. Annual mean free cellulose concentrations within
29 PM₁₀ ranged from 29 ± 38 ng m⁻³ at Bern (urban site) to 284 ± 225 ng m⁻³ at Payerne (rural
30 site). Concentrations were considerably higher during episodes, with spikes exceeding 1150
31 and 2200 ng m⁻³ at Payerne and ANDRA-OPE (rural site), respectively. A clear seasonality,
32 with highest cellulose concentrations during summer and autumn, was observed at all rural and
33 some urban sites. However, some urban locations exhibited a weakened seasonality.
34 Contributions of cellulose-carbon to total organic carbon are moderate on average (0.7 - 5.9
35 %), but much greater during 'episodes', reaching close to 20% at Payerne. Cellulose



36 concentrations correlated poorly between sites, even a ranges of about 10 km, indicating the
37 localised nature of the sources of atmospheric plant debris. With regards to these sources,
38 correlations between cellulose and typical biogenic chemical tracers (polyols and glucose)
39 were moderate to strong (R_s 0.28 – 0.78, $p < 0.0001$) across the nine sites. Seasonality was
40 strongest at sites with stronger biogenic correlations, suggesting the main source of cellulose
41 arises from biogenic origins. A second input to ambient plant debris concentrations was
42 suggested via resuspension of plant matter at several urban sites, due to moderate cellulose
43 correlations with mineral dust tracers, Ca^{2+} and Ti metal (R_s 0.28 – 0.45, $p < 0.007$). No
44 correlation was obtained with the biomass burning tracer (levoglucosan), an indication that this
45 is not a source of atmospheric cellulose. Finally, an investigation into the interannual variability
46 of atmospheric cellulose across the Grenoble metropole area was completed. It was shown that
47 concentrations and sources of ambient cellulose can vary considerably between years. All
48 together, these results deeply improve our knowledge on the phenomenology of plant debris
49 within ambient air.

50

51 **1. Introduction**

52 Ambient aerosols are a key component of our atmospheric system, with complex compositions
53 arising from multiple sources and formation mechanisms. These airborne particles (or
54 particulate matter, PM) have both climatic and health effects which remain poorly understood
55 (Boucher et al., 2013). Particulate matter is made up of elemental and inorganic material, as
56 well as a significant proportion of material of a carbonaceous nature (organic carbon, OC, and
57 elemental carbon, EC) (Franke et al., 2017; Yttri et al., 2007a; Putaud et al., 2004a). PM
58 contains an important portion of organic matter (OM), the chemical composition of which
59 remains largely unidentified (Putaud et al., 2010). In the majority of studies, at most 20% of
60 the OM can be speciated and quantified at the molecular level (Michoud et al., 2021; Alfara
61 et al., 2007). Understanding the sources and atmospheric mechanisms of this OM fraction
62 remains key to uncovering more knowledge of its climatic and health effects, on both local and
63 larger scales (Nozière et al., 2015). Indeed, it has been hypothesised that our current
64 understanding does not account for a number of hidden sources and processes of PM
65 (Karagulian et al., 2015; Wagenbrenner et al., 2017; Klimont et al., 2017).

66

67 A large proportion of research in the last two decades has been focussed on the production of
68 secondary organic aerosol (SOA) arising from the processing of volatile organic compounds



69 (VOCs), or intermediate/semi-volatile ones (I/SVOCs). So far, a smaller effort has been made
70 to account for the potential additional input from primary biological aerosol particles (PBAP –
71 also known as Primary Biogenic Organic Aerosol, PBOA). However, the limited number of
72 available studies show that a significant portion of OM can be associated with such biogenic
73 emissions (Alves, 2017; Liang et al., 2015; Samaké et al., 2019a). PBAP are emitted directly
74 into the atmosphere from the source material, and are described as “solid airborne particles
75 derived from biological organisms, including microorganisms and fragments of biological
76 materials such as plant debris and animal dander” (Fuzzi et al., 2006; Després et al., 2012).
77 PBAP aerodynamic diameters can vary greatly based on the source: ranging from a few
78 nanometres (e.g. viruses and cell fragments), to $> 100 \mu\text{m}$ (plant debris, fungal spores, pollen)
79 (Pöschl, 2005). In terms of their atmospheric significance, some forms of PBAP have been
80 shown to be very efficient ice nuclei and giant cloud condensation nuclei, in regions where
81 anthropogenic sources do not dominate emissions (Pöschl, 2010; Rosenfeld et al., 2008).
82 Biological particles have also been linked with acute respiratory effects (e.g. asthma), allergies,
83 and cancer (Peccia et al., 2011). Estimations of global PBAP natural emissions are in the broad
84 range of 50 – 1000 Tg/yr, while global anthropogenic emissions of PM_{10} via road transport, for
85 instance, amount to about 3.3 Tg/yr (Klimont et al., 2017), highlighting the need for further
86 studies to produce more precise estimates (Jaenicke, 2005; Penner et al., 2001).

87

88 Characterisation of PM can be simplified with the use of chemical tracers (also referred to as
89 molecular markers) as proxy species. Such species should be persistently emitted from a given
90 source and sufficiently stable in the atmosphere to be characterised and quantified. The use of
91 these tracers can also lead to more constrained source apportionment calculations, owing to
92 decreased uncertainties and a stronger statistical output, together with a better understanding
93 of the emission processes (Borlaza et al., 2021; Weber et al., 2019; Waked et al., 2014).
94 Cellulose is considered a good tracer of plant debris, a fraction of the PBAP (Kunit and
95 Puxbaum, 1996; Tenze-Kunit and Puxbaum, 2003; Sánchez-Ochoa et al., 2007).

96

97 Plant debris (e.g. air-dispersed seeds or plant fragments via abrasion or decomposition
98 mechanisms is indeed suspected to be a major contributor to PBAP within the atmosphere
99 (Winiwarter et al., 2009; Graham et al., 2003; Martin et al., 2010; Bozetti et al., 2016; Yttri
100 et al., 2011b). Cellulose is used as a molecular marker in order to quantify the total ambient
101 concentrations of plant debris (Sánchez-Ochoa et al., 2007; Butler and Bailey, 1973). However,
102 where studies around other molecular markers are more prominent, both within the primary



103 biogenic fraction and other classes of aerosol, the number of campaigns investigating
104 measurements of atmospheric cellulose are scarce and cover insufficient ambient conditions
105 (Alves, 2017, and references therein). This remains a concern, especially considering that
106 contributions of cellulose-derived carbon (cellulose-C) to overall organic carbon in the
107 atmosphere can be significant during some periods of the year (Sánchez-Ochoa et al., 2007;
108 Caseiro, 2008).

109

110 Cellulose is present as two forms within global flora: firstly as “free cellulose”, and also as
111 cellulose embedded in lignin or hemicellulose. This portion of cellulose bound to lignin
112 requires an additional delignification process before quantification in atmospheric PM, which
113 requires harsh conditions and long reaction times (Gelencsér, 2004). A conversion from free
114 to total cellulose concentrations was created by Tenze-Kunit and Puxbaum (2003), where free
115 cellulose was shown to contribute 72% of total cellulose abundance. This conversion presents
116 large uncertainties, as it was developed using a very limited sample size ($n < 10$). Nevertheless,
117 free cellulose is commonly used as the proxy species for atmospheric plant debris. Of the few
118 previous characterisation studies to have taken place, contradicting insights into the seasonal
119 variations of cellulose concentrations have been offered (Yttri et al., 2011a; Sánchez-Ochoa et
120 al., 2007; Caseiro, 2008; Yttri et al., 2011b). For example, Sánchez-Ochoa et al. (2007)
121 highlighted a strong pattern of cellulose concentration maxima during spring and summer,
122 excluding their maritime sampling sites, and yet Caseiro (2008) found winter maxima at close
123 to half their monitoring locations. Reasons for this stark contrast are not fully understood.

124

125 This lack of clarity regarding cellulose characterisation of concentrations, seasonal cycles,
126 sources, and emissions processes calls for further measurements. This would enable a better
127 comprehension of the importance of this fraction of PBOA in atmospheric PM. In this study,
128 we present a multi-seasonal investigation of cellulose concentrations alongside other chemical
129 tracers in ambient aerosol, collected at nine sites across both France and Switzerland. The
130 objective of the study was to investigate the seasonal and geographical variability of
131 atmospheric cellulose across sites of varying characteristics. Contributions of cellulose to the
132 OM fraction of PM, and correlations of cellulose with tracers of characteristic sources were
133 also completed, as well as an interannual study of cellulose concentrations at three sites within
134 the Grenoble (France) conurbation. This study, with the gathering of one of the largest data
135 bases on atmospheric cellulose with more than 1500 samples, aims to provide a better
136 understanding of this understudied component of atmospheric PM.



137 **2. Experimental**

138 **2.1 Sampling Sites**

139

140 PM samples used for the present study have been collected during three distinct projects, which
141 are described in the following. The locations of the corresponding measurement sites are
142 presented on Fig. 1a and b, while site classifications, sampling periods, and numbers of
143 available samples are summarised in Table 1 and Table 2.

144

145 The first measurement campaign (QAMECS) focused on the PM₁₀ loading and composition
146 at various sites within the Grenoble metropole (France), as part of the Mobil'Air air quality
147 programme (Borlaza et al., 2021a,b). In these campaigns, three sites were monitored over two
148 one-year periods (2017 – 2018, 2020 – 2021). As the largest metropolis in the Alps, Grenoble
149 is home to around 450,000 inhabitants. The city itself is situated within an alpine valley: the
150 centre is at relatively low altitude (between 200 and 600 metres above sea level) and is
151 surrounded by multiple separate mountain ranges, namely Chartreuse (to the north),
152 Belledonne (east) and Vercors (south and west). These ranges heavily inhibit horizontal air
153 movement, leading to unique meteorological conditions and favouring the formation of
154 temperature inversions, trapping pollutants within the valley, especially during winter. During
155 this study, a PM₁₀ sampling campaign was undertaken in the Grenoble metropole at three sites,
156 each representing a different urban site typology: Les Frênes (LF, urban background), Vif
157 (peri-urban) and Caserne de Bonne (CB, urban centre). All three sites are within 15 km of one
158 another (Fig. 1b).

159

160 Secondly, PM₁₀ and PM_{2.5} samples could be obtained from a monitoring campaign at the
161 Observatoire Pérenne de l'Environnement (ANDRA-OPE), in northern France
162 (<http://ope.andra.fr/index.php?>). Samples have been collected continuously for about a decade
163 at this site (Golly et al., 2019; Borlaza et al., 2021c) but cellulose measurements were
164 conducted and presented in this work for the years 2016, 2017 and 2020, only. PM₁₀ and PM_{2.5}
165 samples were taken on alternate days. The ANDRA-OPE site is situated 230 km east of Paris,
166 on a rise in between lows of the Paris Basin and the mountains in the department of Les Vosges
167 (OPE-ANDRA Atmospheric Station). It is subject to persistent westerly prevailing winds and
168 is surrounded by significant agricultural activities but is notably distant from towns (> 25 km)
169 and small villages (> 4 km).



170 Last but not least, simultaneous PM₁₀ and PM_{2.5} filter samples were taken across five sites in
171 Switzerland, as part of an EMPA monitoring campaign (Grange et al., 2021). These sites varied
172 in characteristics and were sampled for one year (from June 2018 to May 2019). Two rural
173 sites, Magadino and Payern, are included within the study. The former is located south of the
174 Alps, whilst the latter is found on the Northern plateau roughly 50 km from the nearest city of
175 Bern. Filter samples were also taken from urban sites within three of the most populous cities
176 in Switzerland: Basel, Bern and Zurich. Zurich has a similar topography to the Grenoble
177 metropole, whilst the traffic-impacted site in Bern resides within a ‘street canyon’, thus both
178 sites may also experience inhibited air movement. The monitoring site in Basel is within a
179 suburban area, located in an open and park-like environment. It is not expected to be impacted
180 by accumulation effects.
181

Table 1: Sampling period and site characteristics for the PM₁₀ sampling campaign. LF = Les Frênes, CB = Caserne de Bonne. LF, CB and VIF represent sites from the Grenoble metropole.

Site	PM Size, μm	Site Type	Sampling Start	Sampling Finish	# Samples
LF	10	Urban	28/02/2017	31/03/2018	286
		Background	02/01/2020	12/03/2021	
Vif	10	Peri-urban	28/02/2017	31/03/2018	218
			30/06/2020	12/03/2021	
CB	10	Urban	28/02/2017	10/03/2018	209
			30/06/2020	12/03/2021	
ANDRA-OPE	10	Rural background	04/01/2016	27/12/2017	174
			04/01/2020	29/12/2020	
Zurich	10	Urban	03/06/2018	29/05/2019	88
Payerne	10	Rural	03/06/2018	29/05/2019	90
Basel	10	Suburban	03/06/2018	29/05/2019	90
Magadino	10	Rural	03/06/2018	29/05/2019	90
Bern	10	Urban-traffic	03/06/2018	29/05/2019	89

Table 2: Sampling period and site characteristics for the PM_{2.5} sampling campaign

Site	PM Size / μm	Site Type	Sampling Start	Sampling Finish	# Samples
ANDRA-OPE	2.5	Rural Background	01/01/2020	26/12/2020	51
Zurich	2.5	Urban	03/06/2018	29/05/2019	89
Payerne	2.5	Rural	03/06/2018	29/05/2019	90

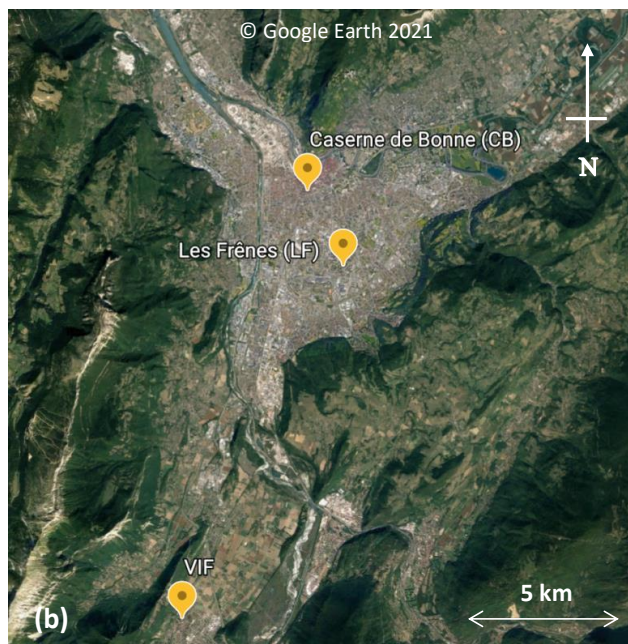
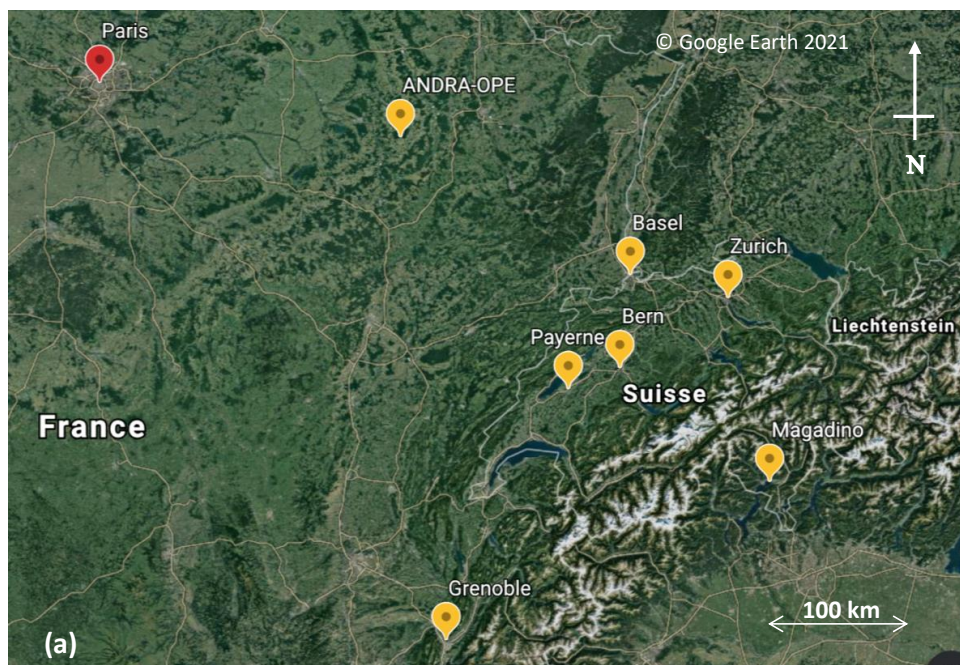


Figure 1. a) A map of all sampling sites from within the study (highlighted with yellow pin drops). Five sites are sampled within Switzerland, three sites within the Grenoble metropole, and one in Northern France – ANDRA-OPE. b) Situation of the three sampling sites within Grenoble.



182 2.2 Sampling Procedure

183

184 At each of the nine sites used for the present study, daily (24-h) PM sample collection periods
185 were conducted according to Table 1 and Table 2 (starting at 00:00 or 09:00 local time) with
186 an average 3-day sampling interval within the Grenoble metropole, 4-day interval for the Swiss
187 sites, and 6-day for the ANDRA-OPE monitoring site. Additional samples for PM₁₀ were
188 collected daily during 9 weeks in summer 2017 in OPE and Grenoble and measured for
189 cellulose, but are not considered in this study (Samaké et al., 2020). The PM collection was
190 performed using high volume samplers (Digitel DA80, 30 m³ h⁻¹) onto 150 mm-diameter pure
191 quartz fibre filters (Tissu-quartz PALL QAT-UP 2500 diameter 150 mm). Excluding the Swiss
192 sites, filters were pre-fired at 500 °C for 12 hours before use to avoid organic contamination,
193 and all were handled under strict quality control procedures. After collection, samples were
194 wrapped in aluminium foil or sterile parchment, sealed in Ziploc plastic bags, and stored at <
195 4 °C until use for chemical analyses. Blank filters were collected to determine detection limits
196 (DL) and to check for the absence of contamination during sample transport, setup, and
197 recovery.

198

199 2.3 Set of Analyses

200

201 All PM₁₀ filters from the nine monitoring locations were analysed for cellulose, while PM_{2.5}
202 filter samples have been analysed at three of the monitoring locations available. The PM₁₀ and
203 PM_{2.5} filter samples were subjected to several other chemical analyses in order to quantify their
204 major chemical components and tracers used in this study.

205

206 Carbonaceous Aerosol

207 Organic carbon (OC) and elemental carbon (EC) were analysed with a Sunset Lab analyser
208 following the EUSAAR2 thermo-optical protocol (Aymoz et al., 2007; Birch and Cary, 1996;
209 Cavalli et al., 2010) and according to the recommendations of EN 16909 European standard.
210 A punch of 1.5 cm² was used and automatic split time was always selected in order to
211 differentiate between EC and OC.

212

213 Sugar alcohols, anhydrides and glucose

214 Sugar anhydrides (levoglucosan, mannosan and galactosan), sugar alcohols (mannitol, arabitol
215 and sorbitol) and glucose were analysed by High Performance Liquid Chromatography with



216 Pulsed Amperometric Detection (HPLC-PAD) (Waked et al., 2014; Samaké et al., 2019a). A
217 Thermo-Fisher ICS 5000⁺ HPLC was used with a 4 mm diameter Metrosep Carb 2×150 mm
218 column and 50 mm pre-column in isocratic mode with an eluent of 15% of sodium hydroxide
219 (200 mM), sodium acetate (4 mM) and 85% water, at 1 mL min⁻¹. For this analysis, an
220 extraction was performed upon 5.09 cm² punches soaked in 7 mL of ultra-pure water under
221 vortex agitation for 20 minutes. The extract was then filtered with a 0.25 μm porosity Acrodisc
222 (Milipore Millex-EIMF) filter before analysis.

223

224 Ionic components

225 Quantification of sodium (Na⁺), ammonium (NH₄⁺), potassium (K⁺), magnesium (Mg²⁺),
226 calcium (Ca²⁺), chloride (Cl⁻), nitrate (NO₃⁻), sulfate (SO₄²⁻), and methane sulfonic acid (MSA)
227 was completed using ion chromatography (IC), in agreement with EN 16913. An extraction
228 was performed on 11.34 cm² filter punches in 10 mL of ultra-pure water under vortex agitation
229 for 20 minutes. The extract was then filtered with a 0.25 μm porosity Acrodisc (Milipore
230 Millex-EIMF) filter. The major ionic components were measured by ion chromatography (IC)
231 following a standard protocol described in Jaffrezo et al. (1998) and Waked et al. (2014) using
232 an ICS3000 dual channel chromatograph (Thermo-Fisher) with AS11HC column for the anions
233 and CS12 for the cations.

234

235 Major and trace elements

236 Preparation of an extract was completed via mineralisation of a 38 mm diameter filter punch
237 in 5 mL of HNO₃ (70%) and 1.25 mL of H₂O₂ at 180 °C for 30 minutes in a microwave oven
238 (microwave MARS 6, CEM). The analysis of 18 elements (Al, As, Ba, Cd, Cr, Cu, Fe, Mn,
239 Mo, Ni, Pb, Rb, Sb, Se, Sn, Ti, V, and Zn) was performed on each filter extract using
240 inductively coupled plasma mass spectroscopy (ICP-MS) (ELAN 6100 DRC II PerkinElmer
241 or NEXION PerkinElmer) akin to the method described by Alleman et al. (2010).

242

243 Cellulose

244 The concentration of “free” cellulose within the filter samples was determined following an
245 improved protocol based on the enzymatic procedure proposed by Kunit and Puxbaum (1996).
246 Free cellulose was extracted in an aqueous solution, which was then enzymatically hydrolysed
247 to glucose units using two cellulolytic enzymes. The glucose concentration was then quantified
248 by using an HPLC-PAD method. The hydrolysis step was the same as originally proposed,
249 however the enzyme quantities and analytical step have been modified in our protocol.



250

251 First, a 21 mm diameter punch was soaked in 3 mL of aqueous solution with a thymol buffer
252 (pH 4.8, see supplementary information) and was extracted for 40 minutes in an ultrasound
253 bath. The two enzymes are added into the solution containing the filter: cellulase (from
254 *Trichoderma reesei*, Sigma Aldrich, C2730) with 20 μL of an aqueous solution at 70 units g^{-1}
255 and glucosidase (from *Aspergillus niger*, Sigma Aldrich, 49291), with 60 μL of an aqueous
256 solution at 5 units g^{-1} . The filter-containing solution was then incubated at 50 °C for 24 hours
257 for hydrolysis to occur. Hydrolysis was then terminated by denaturing the enzymes, by placing
258 the solution in an oven at 100 °C for 45 minutes. Finally, the solution was centrifuged (9000
259 rpm) for 15 minutes at 15 °C and carefully separated and extracted from the filter and enzymes,
260 before being analysed with an HPLC-PAD instrument.

261

262 The HPLC-PAD (Dionex DX500) was equipped with a Metrohm column (250 mm long, 4 mm
263 diameter), with an isocratic run of 40 minutes with the eluents A (84%, H_2O), B (14%, 100
264 mM NaOH), and C (2%, 100 mM NaOH + 150mM NaOAc). Column temperature was
265 maintained at 30 °C. Eluent flow rate was 1.10 mL min^{-1} , and injection volume was 250 μL .
266 Each analytical batch contained six glucose and six cellulose hydrolysis standard solutions,
267 alongside unknown samples. Cellulose standards are used to calculate the cellulose-to-glucose
268 hydrolysis efficiency for each batch and are made from cellulose beads of 20 μm (Sigma
269 Aldrich, S3504). The final calculation of the atmospheric concentration of the free cellulose
270 takes this efficiency of conversion into account. The efficiency was variable between batches,
271 but was typically between 75 – 94%, resulting in an average of $85 \pm 8 \%$. The calculation also
272 subtracts the initial concentrations of atmospheric glucose of each sample, determined in
273 parallel with the aforementioned analysis of sugars and polyols. Finally, field and procedural
274 blanks are taken into account. The procedural blank results are greatly improved when the stock
275 cellulase enzyme solution is filtered to lower their glucose content. This is performed through
276 a series of centrifugal cleaning steps ($n=10$) by tangential ultrafiltration in a Vivaspin 15R tube
277 at 9000 rpm in Milli-Q water. Additional procedural information can be found in the
278 supplementary information (SI).

279 **2.4 Cellulose Method Validation**

280 This novel cellulose quantification method was subjected to a repeatability test, in order to
281 quantify the uncertainties with respect to glucose content within the filter punches. Briefly, a



282 high-volume sampler (Digitel DA80, $30 \text{ m}^3 \text{ h}^{-1}$) was used to collect PM_{10} onto a pre-fired quartz
283 fibre filter (Tissu-quartz PALL QAT-UP 2500 diameter 150 mm) on the roof of the laboratory,
284 and sampled a total of 615.1 m^3 of air on 15/03/2021. Ten filter punches of 21 mm were then
285 taken and subjected to the same cellulose-to-glucose enzymatic procedure as for normal
286 samples. It is important to state that we assume constant concentrations of both native glucose
287 and cellulose within the filter, as well as the same enzymatic cellulose-to-glucose conversion
288 efficiency for all ten filter punches. Each filter punch was then analysed three times using the
289 same HPLC-PAD method, to monitor repeatability in terms of both cellulose hydrolysis and
290 PAD glucose concentration measurements. Post hydrolysis, the total glucose content of the ten
291 filters was found. The variability (Relative Standard Deviation – RSD) was small, ranging from
292 $0.7 - 5.7 \%$ for the three repeats of the same filter sample. The RSD of the glucose content
293 within the ten filter punches was calculated to be 9.9% . For a 95% confidence in the
294 uncertainty estimate, the uncertainty in the measurement was therefore found to be 20% at a
295 maximum.

296

297 **2.5 Limit of Quantification**

298

299 In order to check for potential contamination of filters during transport, sampling and storage,
300 blank filters were taken across the nine sites. Within the Grenoble metropole, blank filters were
301 taken at Les Frênes and then applied to Caserne de Bonne and Vif (labelled QAMECS in Table
302 3). Further, blanks filters were taken at ANDRA-OPE on both PM_{10} and $\text{PM}_{2.5}$ sampling days.
303 With regards to the Swiss sites (EMPA), blanks were taken from each sampling site and an
304 average glucose concentration taken from across the five locations.

305

306 Glucose concentrations calculated in the blanks were then subtracted from measured glucose
307 concentrations within each sample. After, any sample that then yielded a negative
308 concentration of glucose was deemed to be lower than the quantification limit ($< \text{QL}$),
309 representing 5.2% of all samples. Table 3 summarises the concentrations of cellulose on the
310 blank filters, which has been converted from the blank glucose concentration and the average
311 sampling volume taken across the series. QL varied according to the site, from 0.53 to 13.4 ng
312 m^{-3} . In subsequent analyses of monthly, seasonal or annual concentrations (sections 3.1 - 3.3
313 and 3.6), any sample that was deemed $< \text{QL}$ was assigned a cellulose concentration of
314 $[\text{Blank}]/2$. This prevents an artificial increase in average cellulose concentrations.



Table 3: Cellulose concentrations derived from blank filters to derive the quantification limit (QL) for each site.

Campaign	QAMECS			EMPA				ANDRA-OPE	
Site	LF	CB	VIF	Basel	Bern	Magadino	Payerne	Zurich	ANDRA
Blank conc ⁿ , ng m ⁻³	7.1	7.1	7.1	0.53	0.53	0.53	0.53	0.53	13.4
No. Field Blanks	3	3	3	5	5	5	5	5	2
No. Samples < QL	14	16	32	14	3	0	0	0	3
% Samples < QL	4.9	7.7	14.7	15.6	3.4	0	0	0	1.7

315 3. Results and Discussion

316

317 In the following, cellulose concentrations are reported as “free” cellulose. The multiplication
318 factor of 1.39 derived by Tenze-Kunit and Puxbaum (2003) could have been used to derive
319 “total” cellulose. We chose not to do this, due to the large uncertainty in this ratio. From this
320 point onwards, “free” cellulose will be regarded as cellulose.

321

322 3.1 Comparison with previous data from the literature

323

324 Figure 2 illustrates the annual averages of cellulose concentrations across our nine sites (in
325 orange), as well as previous data from the literature (in blue), sorted by site typology and
326 sampled particle size. The bars represent either annual cellulose averages (if sampling lasted
327 greater than one year) or cellulose averages for the designated sampling period. We believe
328 that the roughly 4440 samples (excluding the ones produced within our study) considered in
329 this literature survey represent the near complete data base of cellulose concentrations in PM
330 available in the literature. A tabulated version of the results from within the study can be found
331 in Table 4. An expanded version of Table 4, also including previous literature results, can be
332 found in Table S1 (SI). The evolution of cellulose concentrations across the respective
333 sampling periods for our study have further been included in the SI (Fig. S1).

334

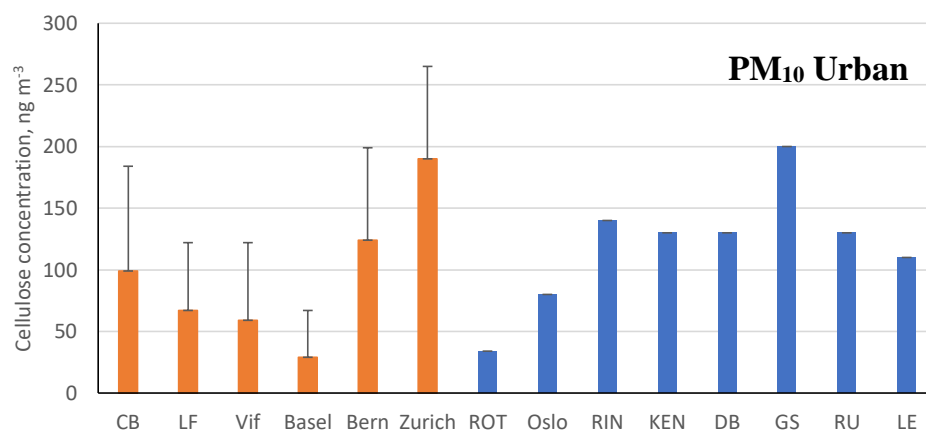
335 The concentrations measured in this study are in the same order of magnitude as those reported
336 in the literature for previous measurement campaigns. This is generally the case for both
337 seasonal averages and overall maximum concentrations, in both coarse and fine mode aerosol
338 (Yttri et al., 2011a; Sánchez-Ochoa et al., 2007; Caseiro, 2008; Yttri et al., 2011b). As shown
339 in Fig. 4, annual cellulose concentrations in PM₁₀ in our study ranged from 29.3 ± 38.4 ng m⁻³



340 (Bern) to $284.3 \pm 224.8 \text{ ng m}^{-3}$ (Payerne), and in $\text{PM}_{2.5}$ ranged from $15.9 \pm 15.0 \text{ ng m}^{-3}$
341 (ANDRA-OPE) to $118.1 \pm 76.5 \text{ ng m}^{-3}$ (Payerne). This annual average PM_{10} cellulose
342 concentration taken at Payerne is higher than any previously recorded in literature by roughly
343 50 ng m^{-3} .

344

345 Moreover, results obtained at Payerne evidenced three episodic (high cellulose concentration)
346 spikes (03/06, 13/07, and 29/07 – highlighted in red, Fig. S1) which exceeded any maximum
347 episode found in literature, by at least 160 ng m^{-3} (Sánchez-Ochoa et al., 2007; Caseiro, 2008;
348 Winiwarter et al., 2009). One striking feature of the overall concentration evolution at Payerne
349 is the high cellulose concentrations at the beginning in June 2018, and the surprisingly low
350 concentrations in April and May 2019 (Fig. S2). Another high concentration episode exceeding
351 those found in literature was documented at the rural site of ANDRA-OPE. The episodic
352 concentration of 2027 ng m^{-3} (07/07/2018 – highlighted in red, Fig. S1) is almost double that
353 of any other measurement, including those generally obtained in the present study. Samaké
354 et al., (2020) recently reported at the same site a noticeable increase in concentrations of PBAP
355 tracers, cellulose included, during harvest in the late summer 2017. However, given the
356 concentration spike in 2018 originated during early July, the middle of the European summer,
357 it is not sure that this new episode can be correlated with agricultural activity.



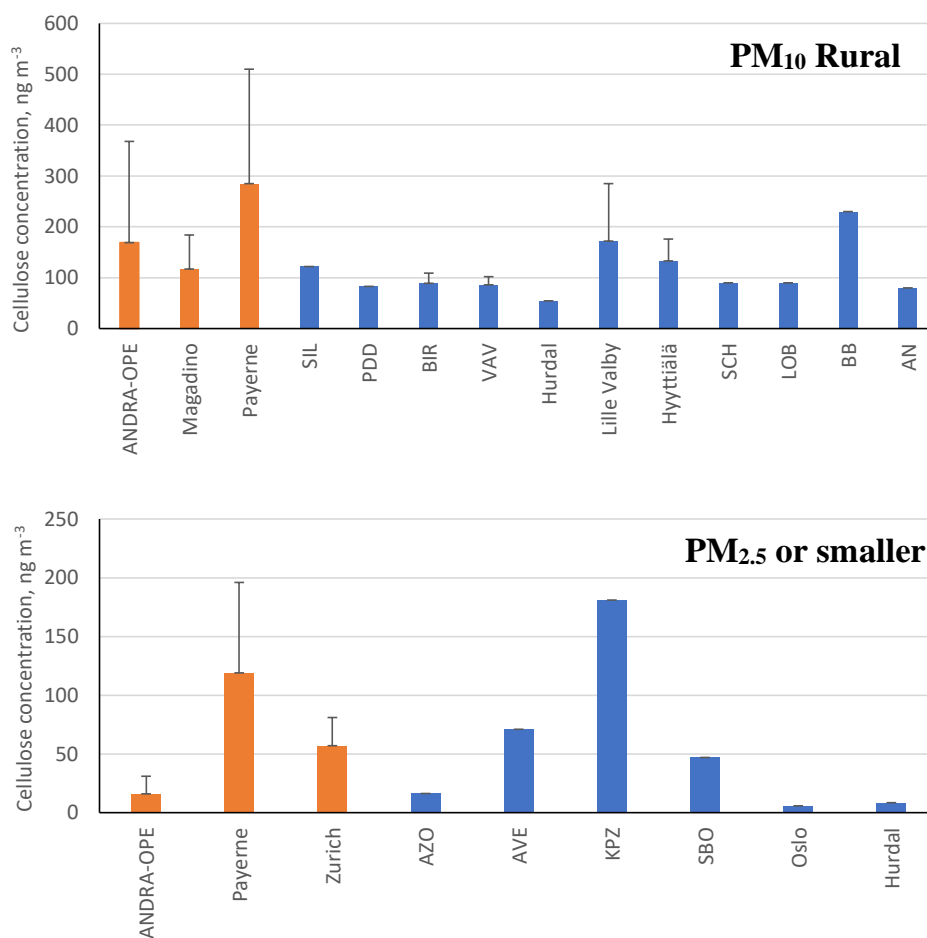


Figure 2: Annual cellulose concentrations (ng m^{-3}) reported within this study (orange bars) alongside previous literature measurements (blue bars). Black bars represent the standard deviation of the results. Bar charts are assigned as follows: Top – urban-based sites; Middle – rural-based sites; Bottom – $\text{PM}_{2.5}$ cellulose measurements (fine mode) or smaller. Note: The locations of all sites taken from literature (blue bars) are summarised in Table S1 (SI), and only positive error bars are used for clarity.



Table 4: Cellulose concentrations (ng m^{-3}) within PM_{10} and $\text{PM}_{2.5}$ across the nine locations studied. Concentrations are shown as annual and seasonal averages (plus 1 σ), as well as the total range of cellulose concentrations seen across the respective period.

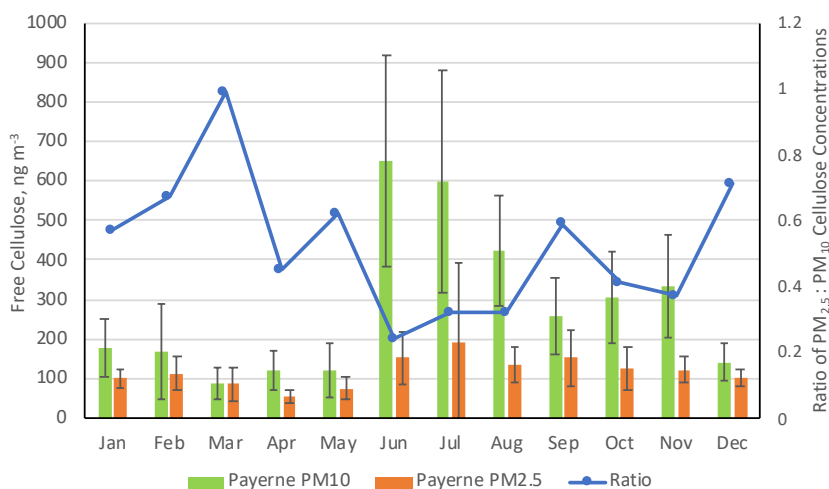
Site	Particle Size (μm)	Annual		Winter		Spring		Summer		Autumn	
		Mean \pm SD	Range	Mean \pm SD	Range	Mean \pm SD	Range	Mean \pm SD	Range	Mean \pm SD	Range
LF	10	67 \pm 55	(1 – 379)	34 \pm 29	(1 – 146)	57 \pm 44	(1 – 214)	98 \pm 58	(29 – 379)	93 \pm 60	(1 – 333)
VIF	10	59 \pm 63	(0.0 – 344)	43 \pm 47	(0.0 – 222)	44 \pm 38	(3 – 186)	68 \pm 87	(1 – 344)	77 \pm 65	(1 – 286)
CB	10	99 \pm 85	(1 – 701)	85 \pm 111	(1 – 701)	131 \pm 56	(46 – 288)	94 \pm 59	(3 – 238)	95 \pm 85	(3 – 357)
OPE-ANDRA	10	169 \pm 199	(3 – 2027)	90 \pm 115	(3 – 518)	102 \pm 116	(12 – 560)	247 \pm 260	(7 – 2027)	90 \pm 67	(13 – 290)
OPE-ANDRA	2.5	16 \pm 15	(0.3 – 41)	17 \pm 21	(0.3 – 41)	< QL	< QL	15 \pm 12	(6 – 32)	16 \pm 18	(2 – 40)
Basel	10	29 \pm 38	(2 – 266)	27 \pm 57	(2 – 266)	35 \pm 37	(10 – 154)	32 \pm 35	(11 – 179)	23 \pm 16	(3 – 83)
Bern	10	124 \pm 75	(25 – 318)	66 \pm 45	(30 – 159)	76 \pm 52	(25 – 241)	143 \pm 45	(99 – 306)	138 \pm 72	(78 – 318)
Magadino	10	117 \pm 67	(16 – 348)	53 \pm 23	(17 – 103)	84 \pm 48	(43 – 282)	135 \pm 65	(60 – 348)	131 \pm 54	(48 – 279)
Payerne	10	284 \pm 225	(53 – 1194)	163 \pm 84	(90 – 437)	108 \pm 54	(53 – 284)	553 \pm 246	(235 – 1194)	300 \pm 114	(96 – 538)
Payerne	2.5	118 \pm 77	(29 – 678)	105 \pm 29	(71 – 201)	74 \pm 33	(29 – 163)	161 \pm 122	(75 – 678)	132 \pm 52	(74 – 275)
Zurich	10	190 \pm 75	(7 – 521)	189 \pm 48	(116 – 342)	177 \pm 51	(81 – 260)	197 \pm 71	(7 – 330)	198 \pm 112	(48 – 521)
Zurich	2.5	57 \pm 24	(11 – 163)	52 \pm 16	(31 – 89)	52 \pm 26	(13 – 199)	58 \pm 20	(33 – 109)	64 \pm 31	(11 – 163)



358 3.2 Size distribution (PM₁₀ vs PM_{2.5})

359

360 Figure 3 presents the comparative monthly average concentrations of cellulose in PM₁₀ and
361 PM_{2.5} taken at the three sites of Payerne, Zurich, and ANDRA-OPE, respectively (overall
362 concentration evolutions presented in Fig. S2, SI). Cellulose concentrations in PM₁₀ are
363 consistently much higher than those in PM_{2.5}, with annual average in PM_{2.5} representing
364 between 18 and 42 % of that in PM₁₀ for the 3 sites. However, very large fluctuations in this
365 monthly ratio can be observed, particularly for the two rural sites (Payerne and ANDRA-OPE).
366 This is primarily due to changes in PM₁₀ cellulose concentrations, as those within PM_{2.5}
367 remained largely consistent. Further, considering the overall evolution in Fig. S2, episodic
368 PM_{2.5} concentrations still generally remain well below the PM₁₀ cellulose concentrations
369 around the same period. It seems that some process is largely impacting the source strength of
370 atmospheric plant debris within PM₁₀, particularly in the rural sites. In the city of Zurich, the
371 cellulose PM_{2.5}/PM₁₀ ratio remained relatively constant, just like the concentrations
372 themselves.



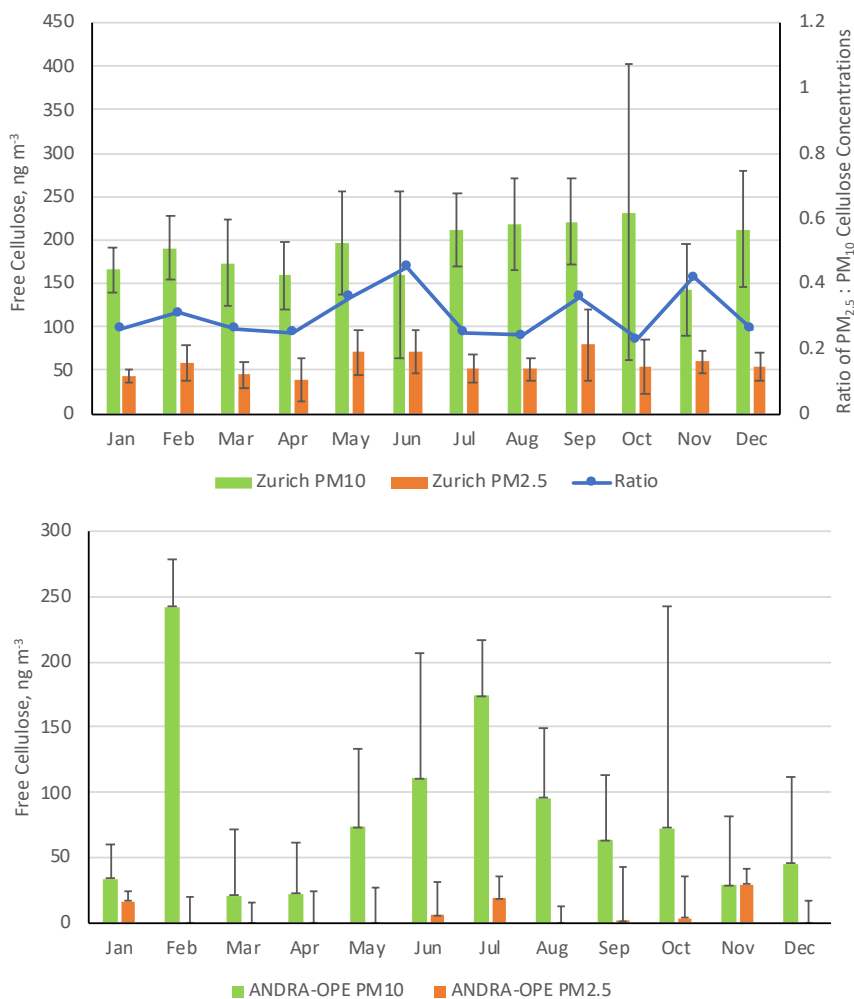


Figure 3: Monthly averages of cellulose concentrations within PM₁₀ (green bars) and PM_{2.5} (orange bars) at the three sampling sites of Payerne (rural, top), Zurich (urban, middle) and ANDRA-OPE (rural, bottom). Black error bars represent one standard deviation of the results. The corresponding blue lines represent the ratio of the monthly mean cellulose concentrations in PM_{2.5} : PM₁₀. **Note: ANDRA-OPE data is only for the year of 2020, and only positive error bars are used for clarity (StDev larger than mean).**

373 Importantly, across the three sites, less than 30% of atmospheric cellulose was found within
374 PM_{2.5}, on average. This large data set of size resolved cellulose concentrations confirms that
375 plant debris predominantly resides within the coarse aerosol mode. Thus, the remainder of this
376 work will solely discuss PM₁₀ data to understand atmospheric cellulose and its behaviour.



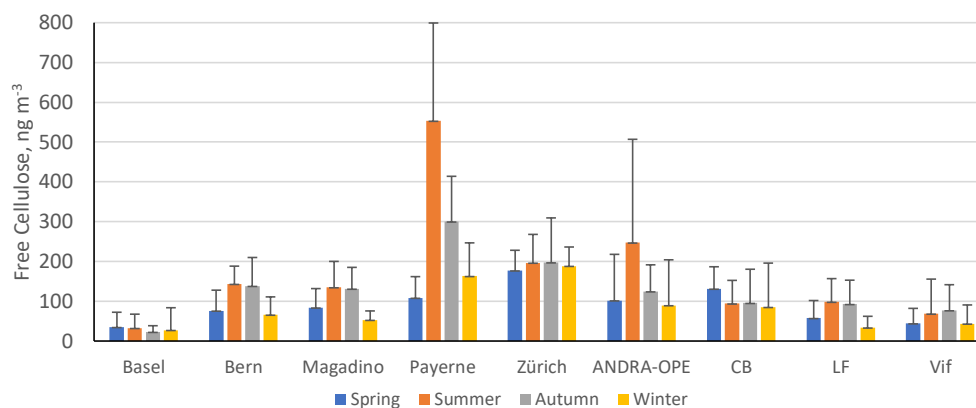
377 **3.3 Variations of cellulose concentrations in time and space**

378

379 Previous studies indicate either a temporal variation with cellulose concentration maxima
380 during the spring and summer seasons (Sánchez-Ochoa et al., 2007), or show very minimal
381 seasonality (Caseiro, 2008). The following discussion will take these observations into account
382 by presenting the results in terms of seasonal averages. Seasons were defined in three-month
383 periods: Dec – Feb (Winter), Mar – May (Spring), Jun – Aug (Summer), Sep – Nov (Autumn).
384 At the nine sites investigated, our PM₁₀ cellulose measurements were above the limit of
385 detection across all seasons. Figure 4 illustrates these seasonal cellulose concentrations (ng m⁻³)
386 for the nine locations. Numerical values of seasonal means and ranges are tabulated as part
387 of Table S1 (SI).

388

389 In general, the seasonal pattern exhibited here shows higher cellulose concentrations during
390 summer and autumn, likely due to higher biological activity granted by increased temperature
391 and humidity (Verma et al., 2018). This is the case at all rural sites, and some urban locations
392 (Bern, LF, Vif). However, the extent to which these concentrations exceed the other seasons
393 varied greatly. Normalised seasonal concentrations for each site can be found in Fig. S3, to
394 show this variability. Considering this general seasonality, a summer-autumn maximum in
395 cellulose concentrations deviates from the spring-summer maximum suggested by Sánchez-
396 Ochoa et al. (2007). This may be a result of the different particle size fractions measured as
397 part of their sampling campaign (i.e., PM₂, PM_{2.5} or PM₁₀), compared to the consistent PM₁₀
398 measurements used in this study. This might also be due to the presence of three high altitude,
399 mountainous sites comprised within the six sites investigated by Sánchez-Ochoa et al. (2007).
400 Large standard deviations are also noticed at the two rural sites of ANDRA-OPE and Payerne,
401 especially during the summer months. This implies a significant variability in the source of
402 atmospheric cellulose at these sites, especially when compared to the more urban locations
403 showing smaller standard deviations and therefore a smaller flux from the cellulose source.



Site	LF	CB	VIF	Basel	Bern	Magadino	Payerne	Zurich	ANDRA-OPE
Classification	Urban Background	Urban centre	Peri-urban	Suburban	Urban-traffic	Rural	Rural	Urban	Rural background

Figure 4: Mean cellulose concentrations (ng m^{-3}) at each site, by season: spring (blue), summer (orange), autumn (grey) and winter (yellow). Black error bars represent one standard deviation of the seasonal averages. Only positive error bars are added, for clarity. Note: LF = Les Frênes; CB = Caserne de Bonne. Grenoble-based sites represented by CB, LF and Vif.

404 Whilst this is the general case, there are notable exceptions. Both the urban centres of Zurich
 405 and CB show very little seasonal variability compared to their more rural counterparts.
 406 Cellulose concentrations in Basel (suburban) also show minimal seasonality, but this may be
 407 due to concentrations being too small to exhibit a full seasonal pattern. This is surprising, given
 408 the close proximity of the site to a park-like area with trees and gardens. The lack of seasonality
 409 in urban settings, however, is consistent with the findings of Caseiro (2008). Additionally,
 410 Caseiro (2008) provided some evidence of cellulose concentrations at urban sites being greater
 411 than for nearby rural or background sites, with residential areas being an intermediate case.
 412 Within our Grenoble-based dataset as a comparison, CB (urban) does indeed exhibit cellulose
 413 concentrations marginally higher than the urban background site of LF and significantly higher
 414 than Vif (peri-urban).

415

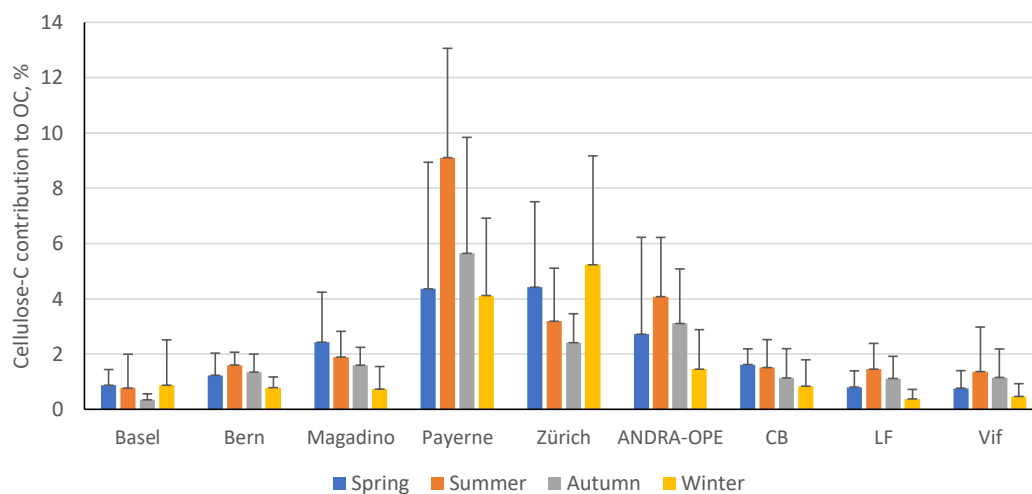
416 Alongside Basel, Caserne de Bonne also deviates from the general trend of summer-autumn
 417 maxima in cellulose concentrations observed across the other seven locations investigated here.
 418 Reasons for this are unclear, but this is suggestive of a source change in atmospheric plant
 419 debris, or an additional source being present at some urban locations, that may mask the typical
 420 seasonality. Given that these locations are urban in character, the weak seasonal variations may
 421 be owing to anthropogenic activity. This will be investigated in section 3.5.



422 3.4 Contribution of Cellulose-C to OC

423

424 To determine the overall importance of cellulose contribution to PM, the percentage
 425 contribution of cellulose-carbon to total organic carbon (Cellulose-C to OC) was determined.
 426 Figure 5 illustrates this seasonal average percentage contribution. Table S5 summarises
 427 numerically the overall average and seasonal percentage contributions and the ratio of
 428 cellulose-C contribution during winter and summer. Also highlighted is the maximum
 429 contribution of cellulose-C to OC experienced over the respective sampling periods at each
 430 site.



Site	LF	CB	VIF	Basel	Bern	Magadino	Payerne	Zurich	ANDRA-OPE
Classification	Urban Background	Urban centre	Peri-urban	Suburban	Urban-traffic	Rural	Rural	Urban	Rural background

Figure 5: Seasonal contributions of cellulose-C to OC (%) in PM₁₀ across the nine sites. Seasons are as follows: Spring (blue) - Mar-May; Summer (orange) - Jun-Aug; Autumn (grey) - Sep-Nov; Winter (yellow) - Dec-Feb. Black error bars represent one standard deviation of the mean values. Only positive error bars are included, for clarity. Note: LF = Les Frênes, CB = Caserne de Bonne. Grenoble-based sites represented by CB, LF and Vif.

431 The highest contributions to OC were typically found at rural sites, potentially due to fewer
 432 local sources of OC in rural sites compared to more urban locations. In fact, the annual
 433 contribution to OC found at Payerne (5.9 ± 4.4 %) is the highest found in literature. However,
 434 the annual average for the urban site of Zurich is also in a high range, at 3.8 ± 2.9 %. Regarding
 435 seasonal contributions, the rural sites in this study show a significantly different seasonal
 436 pattern compared those found in the study by Sánchez-Ochoa et al. (2007). Here, we see a
 437 noticeably smaller contribution of cellulose-C to OC during winter compared to summer. This



438 is reflected in the respective winter/summer ratios of cellulose-C contribution: the values in
439 this study range between 0.36 – 0.45, in comparison to 4.2 and 0.3 at the PM₁₀ rural and high-
440 altitude sites used in their study (Sánchez-Ochoa et al., 2007).

441

442 While seasonal contributions appear to be moderate in most cases, the contribution of cellulose-
443 C within episodes can be much more significant. It is also worth noting that these contributions
444 to OC are derived from free cellulose concentrations. Thus, the contribution to overall OC will
445 be higher when considering total cellulose. At sites with typically lower seasonal contributions
446 (Basel, Bern, LF), the episodic contributions reached between roughly 4.1 to 6.3 %. However,
447 at the sites that illustrated a much higher seasonal average contribution to OC, the maximum
448 contributions during episodes were found to be between 16.1 % at Zurich and 19.7 % at
449 Payerne. These maximum contributions (detailed in Table S5) are similar to those found at the
450 background sites by Sánchez-Ochoa et al. (2007). These values stand to highlight the
451 substantial contribution that atmospheric plant debris can have on atmospheric composition. In
452 other words, PBAP, and plant debris in particular, can contribute greatly to OM and must be
453 considered within all future characterisation and source apportionment studies.

454

455 Lastly, the contribution of coarse mode (PM with diameter less than 10 µm and greater than
456 2.5 µm) cellulose-C to coarse mode OC was evaluated at the three sites that completed both
457 PM₁₀ and PM_{2.5} analysis (ANDRA-OPE, Payerne and Zurich). This can be seen in Table S6,
458 in the SI. As PM_{2.5} data for ANDRA-OPE was only available for the 2020 sampling campaign,
459 PM₁₀ data from 2016 and 2017 was excluded. Table S6 shows a contribution of coarse
460 cellulose-C to be 3.16% at ANDRA-OPE, which is of very similar magnitude to that of the
461 overall cellulose-C contribution to OC. This is potentially due to the significant reduction in
462 cellulose source strength at the ANDRA-OPE site during the year of 2020, compared to the
463 years prior. This will be discussed in section 3.7. However, at both Payerne and Zurich, the
464 annual contributions to coarse OC are notably higher (11.02 % and 13.04 %, respectively) than
465 that of overall cellulose-C to OC (5.88 % and 3.76 %, respectively). From this data, we can see
466 that plant debris makes up a significant component of the coarse fraction of OM within these
467 two datasets.



468 3.5 Investigation of cellulose emission sources

469

470 To further evaluate the potential sources of plant debris into the atmosphere, correlations
 471 between cellulose and other source-specific tracers were investigated. This is the first cellulose
 472 field study to investigate these correlations with other tracers. Briefly, three specific sources
 473 have been hypothesised in the literature: direct biogenic emissions, unpyrolysed cellulose
 474 during biomass burning, and anthropogenic resuspension and milling of plant debris (Yttri et
 475 al., 2011a; Sánchez-Ochoa et al., 2007; Caseiro, 2008; Yttri et al., 2011b). The chemical tracers
 476 used as proxies for these sources in this study are i) glucose and polyols, ii) levoglucosan, and
 477 iii) EC, Ca²⁺ and Ti, respectively. A suite of correlation coefficients (Spearman's rank
 478 correlation, *R_s*) was created for each site to monitor variations in correlations between site
 479 types using daily samples. Spearman's rank correlation was used in this section to better
 480 account for anomalous results between different datasets (e.g. cellulose vs polyols). A value of
 481 1 indicates a perfect positive correlation, and a value of -1 indicates a perfect negative
 482 correlation. Table 5 shows the strength of the cellulose-tracer correlation at individual sites
 483 across the entire sampling period. A full table, inclusive with the number of data points (*n*) and
 484 *p* values for each correlation, plus *R_s* values within each season, can be found in the SI (Table
 485 S7).

*Table 5: Spearman correlations (*R_s*) between cellulose and characteristic chemical tracers across the nine sites. A red cell indicates a positive correlation between cellulose and the selected chemical tracer, whilst a blue cell indicates a negative correlation. A colour-coded key of corresponding *R_s* values is to the right of the table. Grenoble-based sites: CB – Caserne de Bonne, LF – Les Frênes and Vif. Note: polyols = sum of arabitol, mannitol and sorbitol.*

<i>R_s</i>	CB	LF	Vif	Basel	Bern	Magadino	Payerne	Zurich	ANDRA-OPE	
Polyols	0.28	0.60	0.42	0.33	0.61	0.78	0.68	0.43	0.66	1.00
Glucose	0.28	0.57	0.48	0.39	0.63	0.66	0.71	0.43	0.58	0.66
Levoglucosan	-0.06	-0.38	-0.08	0.00	-0.07	-0.37	-0.18	-0.03	-0.43	0.33
EC	0.19	-0.08	0.04	0.34	0.25	-0.03	0.07	0.25	0.11	0.00
Ca ²⁺	0.14	0.28	0.12	0.37	0.45	-0.12	0.21	0.29	0.33	-0.33
Ti	0.28	0.34	0.03	0.40	0.39	0.05	0.31	0.31	0.18	-0.66
										-1.00

Site	LF	CB	VIF	Basel	Bern	Magadino	Payerne	Zurich	ANDRA-OPE
Classification	Urban Background	Urban centre	Peri-urban	Suburban	Urban-traffic	Rural	Rural	Urban	Rural background

486 Biogenic sources

487

488 The best understood chemical tracers for biogenic emissions are polyols (sum of arabitol,
 489 sorbitol and mannitol) and glucose (Zhang et al., 2010; Després et al., 2012; Bauer et al., 2008).



490 Glucose is the most abundant monosaccharide amongst vascular plants, is an important carbon
491 source for bacteria and fungi, and remains stable in the atmosphere (Jia et al., 2010; Zhu et al.,
492 2015). Its multiple biological sources into the atmosphere means that it can provide a good
493 insight as to whether atmospheric plant debris comes from a predominantly biogenic source.
494 Polyols are also used to provide tracer correlations with cellulose. These species are typically
495 used as markers of airborne fungi but have also been found to be present within leaves and
496 pollen (Medeiros, 2006).

497

498 As we can see in Table 5, relatively strong positive correlations arise between cellulose and
499 the two selected biogenic source tracers at most sites. The strongest correlations were seen at
500 rural locations (Magadino, Payerne and ANDRA-OPE, $p < 0.0001$). However, Bern and LF,
501 traffic-impacted and urban background sites respectively, also showed similar R_s magnitudes
502 to their rural counterparts ($p < 0.0001$). This indicates that similar factors promote the emission
503 of all of cellulose, polyols and glucose. The remaining four sites, all urban in character, showed
504 weaker correlations of cellulose with both glucose and polyols. It should also be said that
505 correlations across all sites were of similar magnitude when comparing cellulose-glucose and
506 cellulose-polyol concentrations. The stronger correlations at the rural sites indicate that a
507 significant portion of atmospheric cellulose, and thus plant debris, arises from biogenic sources
508 at these sites. As the values are typically below 0.7, this could suggest a different timing of
509 emissions between biogenic tracers and cellulose (e.g. meteorological conditions favouring
510 emission of fungal spores before plant debris). This is a distinct possibility, given that sampling
511 ranges between 3-6 days at the nine locations. Additionally, these moderate correlations with
512 biogenic tracers could be due to some input from other sources, but of a lower magnitude. By
513 contrast, the weaker correlations observed at most urban sites suggest that there remain other,
514 potentially more prominent, sources at play that determine atmospheric cellulose
515 concentrations. The two exceptions to this, LF and Bern, show that the sources of atmospheric
516 plant debris are not consistent within each designated site type.

517

518 It is noteworthy that the five locations that illustrate the strongest correlations with glucose and
519 polyols are the five out of the six sites in which the common, general-case seasonality is
520 observed. It is thus likely that this typical seasonality pattern is observed where the biogenic
521 source of plant debris is the most dominant.



522 **Biomass Burning**

523

524 A potential second source of atmospheric cellulose was proposed by Sánchez-Ochoa et al.
525 (2007) to account for anomalous high cellulose concentrations during winter. They suggested
526 that they were caused by unburned cellulose during biomass burning (Sánchez-Ochoa et al.,
527 2007). They also concluded that it was an unlikely process, based on the work of Schmidl et
528 al. (2005) illustrating that only a very small concentration of cellulose can be found in wood
529 smoke. Nevertheless, correlations between cellulose and levoglucosan, a chemical tracer for
530 biomass burning, were completed here to provide a more robust understanding of the viability
531 of this hypothesis (Giannoni et al., 2012; Madsen et al., 2018).

532

533 Table 5 indicates cellulose-levoglucosan tracers across all sites show no correlation with one
534 another, and in some instances show a moderate anti-correlation (R_s -0.43 – 0.00, p 0.0001 –
535 0.98). Stronger anti-correlations were seen at sites that also showed strong correlations with
536 biogenic tracers. Given that the theory was based on a winter-time source of atmospheric
537 cellulose via biomass burning, it is important to view the seasonal correlations to gain a fuller
538 understanding (Table S7, SI). Of all sites, the Grenoble-based locations (Caserne de Bonne,
539 Les Frênes and Vif) were the only three to have greater than the thirty data points of
540 simultaneous cellulose and levoglucosan measurements needed for a robust correlation. None
541 of these three locations showed any correlation between cellulose and levoglucosan (R_s 0.05 –
542 0.18, p 0.14 – 0.74). In fact, the remaining six locations showed also very weak correlation,
543 except for the site of Bern, which showed a moderate correlation (R_s 0.49, p < 0.03). But, as
544 already mentioned, the relatively small wintertime dataset for these six other sites (n = 21 to
545 25) does not provide strong confidence in these results. Thus, we can state that the sources of
546 atmospheric plant debris do not include any significant input from biomass burning.

547

548 **Other anthropogenic sources**

549

550 It has also been hypothesised that others anthropogenic activities may contribute to
551 atmospheric cellulose. Caseiro (2008) noticed typically higher cellulose concentrations in
552 urban locations, compared to the more rural ones within their study. The predominant
553 hypotheses for anthropogenic input of plant debris into the atmosphere were mechanisms such
554 as resuspension via road traffic, paper usage, and lawn mowing. To test these hypotheses,
555 correlations were computed between cellulose and known chemical tracers for man-made



556 emissions and mineral dust: Elemental Carbon (EC) and Ti/Ca^{2+} , respectively. EC is a known
557 primary product of combustion processes and is dominated by anthropogenic sources,
558 including road traffic, in urban areas (Wu and Yu, 2016). Ca^{2+} is also used as a tracer for
559 mineral dust, which commonly enters the atmosphere via road wear, gritting and dust
560 resuspension due to transport, as well as via gusts of wind (Denier van der Gon et al., 2010).
561 At the Swiss sites, Ca metal was measured as opposed to the soluble ion Ca^{2+} , but is a still a
562 suitable tracer for mineral dust. Titanium metal is also used as a chemical tracer for mineral
563 dust and thus should possess a similar resuspension mechanism (Charron et al., 2019). A
564 positive correlation with these dust tracers would suggest plant debris is resuspended into the
565 atmosphere via the same established mechanism as mineral dust.

566

567 Considering EC first, Table 5 shows typically weak positive correlations between EC and
568 cellulose abundance at sites considered to be urban or traffic-impacted in character, excluding
569 Les Frênes (R_s 0.25 – 0.34, $p < 0.03$). The rural-based sites showed very little correlation (R_s
570 -0.03 – 0.11, p 0.16 – 0.79), suggesting that any resuspension mechanism of plant debris
571 involving automotive vehicles is only active in more built-up areas. In any case, automotive
572 resuspension of plant debris appears to be relatively weak, even when present at the more urban
573 locations.

574

575 In general, cellulose correlations with the two mineral dust chemical tracers were slightly
576 stronger across all sites compared to their respective cellulose-EC correlations. These values
577 were once again higher at more urban locations compared to rural sites, in particular at Basel
578 and Bern, which show R_s values between 0.37 and 0.45 ($p < 0.001$). The stronger correlations
579 with mineral dust do seem to suggest that ambient cellulose concentrations are somewhat
580 influenced by the resuspension of plant debris in a manner similar to that of mineral dust. Yet,
581 given the lack of significant correlation with EC, it seems that a resuspension mechanism may
582 not include a vehicular input. Other anthropogenic resuspension mechanisms not related to
583 traffic may contribute; paper usage (e.g. newspaper and cardboard production) has been
584 mooted in previous literature (Caseiro, 2008). These still unknown mechanisms could shadow
585 the seasonality of cellulose concentrations in more urban locations. One possible process
586 without anthropogenic input, however, could be via strong gusts of wind that resuspend this
587 plant material. Agricultural activities can also play a large role in emitting plant matter into the
588 atmosphere. Samaké et al. (2019b) showed maximum cellulose concentrations occurred during
589 harvest (summer) at ANDRA-OPE. This agricultural input from harvested land is also a major



590 emission source of polyols and glucose, which may explain the strong correlations of cellulose
591 with these tracers at the more rural locations (Samaké et al., 2019b).

592

593 Overall, several conclusions can be drawn for the three potential sources proposed in the
594 literature. Firstly, the direct biogenic source of atmospheric plant debris is by far the most
595 significant, showing moderate to strong Spearman correlations between cellulose and other
596 characteristic biogenic tracers. This is particularly clear in rural sites; the correlation is
597 inconsistent among other site types. In addition, there is no source of atmospheric plant debris
598 that arises from biomass burning across any season or site type, as already suggested by Borlaza
599 et al. (2021a). Lastly, the resuspension of plant material could be another possible input to
600 overall ambient plant debris abundance. This mechanism does not seem to incorporate road
601 traffic in the way suggested by Caseiro (2008), given the lack of correlation between cellulose
602 and EC abundance.

603

604 **3.6 Local vs. regional origin**

605

606 Seasonal cellulose variations do not show a similar pattern across all sites, nor one that is
607 consistent across different regions and scales. This trend, or lack thereof, was expressed
608 numerically using correlation coefficients (R^2) of monthly concentration averages for the
609 groups of sites that were sampled at the same time. As shown in Table 6, the correlations
610 between sites within the Grenoble metropole (CB, LF and Vif) are low to moderate. This is
611 also the case for the Swiss sites, which span a much larger spatial range compared to the
612 Grenoble-based sites. The lack of a shared temporal variability seems to indicate that the major
613 sources of plant debris are most likely to be local to each site. It may also suggest that several
614 mechanisms impacting ambient cellulose concentrations contribute to different degrees
615 according to the investigated site (Winiwarter et al., 2009; Borlaza et al., 2021; Caseiro, 2008).
616 Moderate correlations between the traffic-impacted location in Bern with the two rural sites of
617 Magadino and Payerne were the highest among the Swiss sites. Regardless, these values are
618 not indicative of a common source. The Grenoble-based sites of LF and Vif do seem to show
619 a slight exception, producing an R^2 value close to 0.7 ($p < 0.0001$). The three monitoring
620 locations within the Grenoble metropole are within 15 km of one another, so a common source
621 of atmospheric plant debris on local scales of this magnitude remains possible.



Table 6: Correlations (R^2) monthly cellulose concentrations between the Swiss sites (top) and between Grenoble-based (bottom) sites (LF, CB and Vif). The colour-coded key (right) gives the corresponding colour of the correlation strength (R^2 values). A strong correlation (R^2 close to 1) is coded red, with no correlation coded blue. Intermediate correlations are coded white. **Note:** CB = Caserne de Bonne, LF = Les Frênes. Grenoble-based sites represented by CB, LF and Vif.

R^2					
Bern	0.0092				
Magadino	0.0059	0.4636			1
Payerne	0.016	0.4275	0.2941		0.8
Zurich	0.0124	0.395	0.1814	0.0046	0.6
		Basel	Bern	Magadino	Payerne
					0.5
					0.4
					0.2
					0

R^2		
CB	0.0056	
VIF	0.6944	0.0172
	LF	CB

622

623

624

625

626

Site	LF	CB	VIF	Basel	Bern	Magadino	Payerne	Zurich
Classification	Urban Background	Urban centre	Peri-urban	Suburban	Urban-traffic	Rural	Rural	Urban

627

628

629

630

631

632

633

634

635

636

637

638

639

640

641

642

643

644

The R^2 values in Table 6 were compared to correlations between monthly mean concentrations of the so-called polyol fraction (i.e., sum of arabitol, mannitol and sorbitol) for the same set of locations (Samaké et al., 2019a; Borlaza et al., 2021a; Grange et al., 2021). In contrast to cellulose, polyols show common temporal variations, with R^2 correlations ranging from 0.4 – 0.91 and 0.95 – 0.98 ($p < 0.0001$) within the groups of Swiss and Grenoble-based sites, respectively (Table S3 and Table S4). Polyols are used as chemical tracers for fungal spores, a very common class of PBAP, and here provide a near perfect example of a PBAP class displaying homogenized concentration variations over time at a regional scale. This suggests a single common source of polyols that is impacted similarly by external factors across all locations, especially at short range e.g. within the Grenoble area. This was also suggested by Borlaza et al. (2021) during their PMF study, and by Samaké et al. (2019a) as part of their study across all of France. Moreover, Samaké et al. (2020, 2021) evidenced that the presence of fungi and bacteria in ambient air is mostly related to a limited number of microorganism species only, which vary from one climatic region to the next.

The stark contrast between the two sets of chemical tracers (cellulose vs. polyols) highlights the rather local nature of atmospheric plant debris and its sources. Given that meteorology is relatively consistent on a short to medium scale (< 200 km), it would be expected that plant



645 debris emissions would impact all sites of a given area similarly. However, heterogeneous
646 distribution of the diverse plant species at the city (or regional) scale might induce specific
647 temporal variations in the emissions of plant debris at the local scale. Therefore, the lack of
648 correlation in cellulose datasets may result from site-to-site differences in the dominant sources
649 (flora) or emission processes of ambient plant debris (Caseiro, 2008).

650

651 **3.7 Interannual Comparison – A Combined Approach**

652

653 Cellulose concentrations were measured over two separate time periods: 2017-18 and 2020-21
654 in Grenoble, and over three separate time periods: 2016, 2017 and 2020 at ANDRA-OPE.
655 These multiple datasets (with a similar number of data points) gave us the opportunity to assess
656 the interannual variations of atmospheric plant debris, in the same regions. This provided the
657 possibility to combine the various analyses used in the above sections as part of a more small-
658 scale, holistic investigation.

659 **Grenoble**

660 Figure 6 presents the seasonal mean cellulose concentrations across the two time periods within
661 the Grenoble metropole (expressed numerically in Table S8, SI). The difference in cellulose
662 concentrations between different sampling years is stark. Both CB and Vif show significant
663 decreases in cellulose concentrations from 2017-18 to 2020-21, with the exception of the spring
664 period. For example, summer and autumn cellulose concentrations decreased by over a factor
665 of 3 between 2017-18 and 2020-21. This is not the case for the urban background site of Les
666 Frênes, where the seasonal concentrations typically increased across all seasons except for
667 spring.

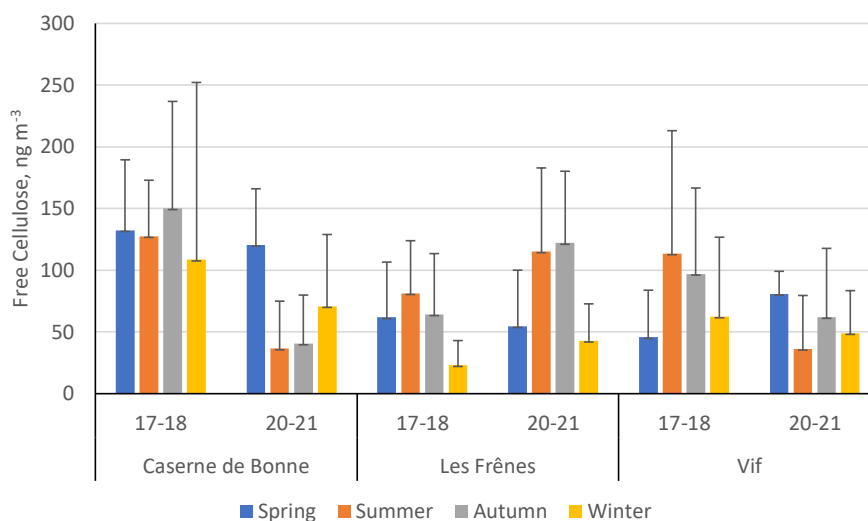


Figure 6: Seasonal mean averages of cellulose concentrations (ng m^{-3}) of the three sites within the Grenoble metropole across the two separate sampling periods: 2017-18 and 2020-21. Black error bars represent one standard deviation of the seasonal means. Only positive error bars are shown to aid clarity. Seasons are defined as: Dec-Feb (winter), Mar-May (spring), Jun-Aug (summer), Sep-Nov (autumn). Site classifications are as follows: Caserne de Bonne – urban; Les Frênes – urban background; Vif – peri-urban.

668 Temperature data was used as an attempt to elucidate the contrasting concentrations across the
669 two sampling periods (Fig. S4, SI). A warmer and more humid climate brings about greater
670 biological activity (e.g. an increase in pollen production), but can also speed up the
671 decomposition processes involved in generating plant debris (Verma et al., 2018; Martínez et
672 al., 2014). Temperature data for Grenoble across the two sampling periods was provided by
673 Atmo Auvergne-Rhône-Alpes (Atmo AURA).

674

675 Seasonal and monthly average temperatures across the two sampling periods show some
676 differences, but the variation is slight (Fig. S4, SI). It is highly unlikely in this instance that the
677 large variations in the atmospheric cellulose concentrations were caused by ambient
678 temperature changes. This is further supported by the lack of change in seasonal average polyol
679 concentrations for the same sites, shown in Fig. S5, whose concentrations are impacted solely
680 by biogenic factors (Zhang et al., 2010; Després et al., 2012; Bauer et al., 2008). While other
681 climate data were not been available, there is potential for the variability in cellulose source
682 strengths to have been caused by factors that are not purely meteorological. This observed
683 variability may be related to changes in human activities, associated with the COVID-19



684 lockdown and sanitary restrictions. This would most profoundly affect the pedestrianised urban
685 centre of Caserne de Bonne, with the prolonged closure of shops in the area surrounding the
686 sampling site, together with the decrease of traffic on the nearby avenues.
687
688 Interestingly, changes in ambient cellulose concentrations across the two periods are
689 concomitant with changes in the contribution of cellulose-C to OC (Fig. 7, numerical values
690 Table S9). Thus, it is likely that changes in atmospheric cellulose concentrations will have
691 resulted from changes in the source strength of plant debris, and not from a wider-scale
692 reduction in some or all other OC sources.

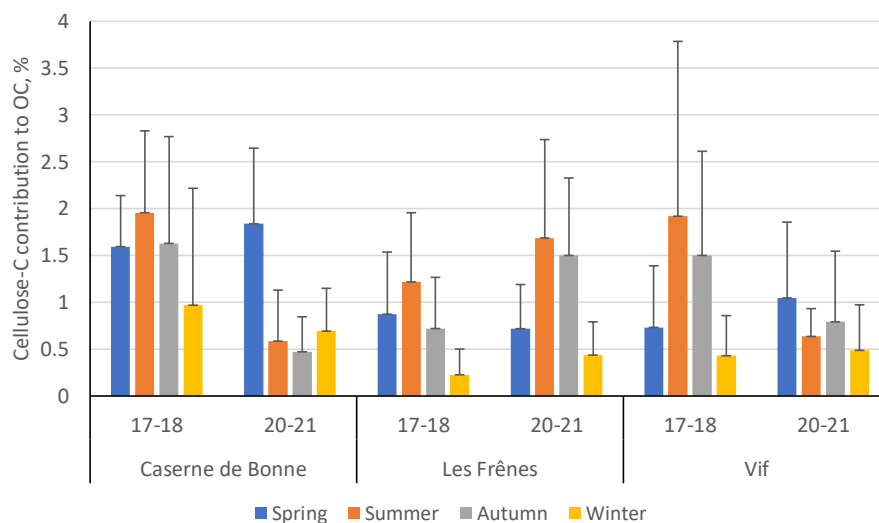


Figure 7: Percentage contribution of cellulose-derived carbon towards overall organic carbon (cellulose-C to OC) across the three sites within the Grenoble metropole during the two separate sampling periods: 2017-18 and 2020-21. Black error bars represent one standard deviation of the seasonal means. Only positive error bars are shown to aid clarity. Seasons are defined as: Dec-Feb (winter), Mar-May (spring), Jun-Aug (summer), Sep-Nov (autumn).

Site classifications are as follows: Caserne de Bonne – urban; Les Frênes – urban background; Vif – peri-urban.

693 Given that these large interannual variations seemed to be predominantly limited to cellulose
694 and not the remaining sources of OC, it was necessary to evaluate the potential sources once
695 more. Following section 3.5, cellulose-tracer correlations were again produced using the same
696 characteristic source tracers for the two periods, to see if changes in cellulose concentrations
697 were consistent with variations in tracer correlations. These correlation coefficients can be seen
698 in Table 7 (Table S10 for full table). From the two sets of correlations, it is evident that the



699 sources of plant debris are only consistent between campaigns at Les Frênes. Reasonable
700 correlations with characteristic biogenic chemical tracers (polyols and glucose) remain
701 consistent, whilst a moderate anti-correlation is still seen between cellulose and levoglucosan.
702 No correlations with EC were seen throughout the two campaigns.

Table 7: Spearman correlations (R_s) between cellulose and characteristic chemical tracers at the Grenoble-based sites, across the two separate sampling periods: 2017-18; 2020-21. A red cell indicates a positive correlation between cellulose and the selected chemical tracer, whilst a blue cell indicates a negative correlation. A colour-coded key of corresponding R_s values is to the right of the table.

Site classifications are as follows: Caserne de Bonne (CB) – urban; Les Frênes (LF) – urban background; Vif – peri-urban. Note: polyols = sum of arabitol, mannitol and sorbitol.

R_s	Grenoble 2017 - 2018			Grenoble 2020 - 2021			
	CB	LF	Vif	CB	LF	Vif	
							1.00
							0.66
							0.33
Polyols	0.46	0.63	0.59	-0.09	0.68	0.22	0.00
Glucose	0.47	0.62	0.66	-0.08	0.56	0.24	-0.33
Levoglucosan	-0.07	-0.48	-0.21	0.25	-0.38	0.10	-0.66
EC	0.15	-0.11	-0.07	0.18	0.01	0.16	-1.00
Ca ²⁺	0.14	0.22	0.00	0.31	0.32	0.32	

703 By contrast, tracer correlations across both CB and Vif vary significantly between the two
704 campaigns. R_s values of cellulose versus glucose or polyol concentrations decrease
705 significantly during the 20/21 campaign. A weak positive correlation becomes apparent
706 between cellulose and Ca²⁺ concentrations during the 20/21 campaign that was absent during
707 the previous series. This is particularly visible at Vif, but it is also a consistent trend across all
708 three sites. These findings suggest potentially two possible hypotheses. Firstly, the contribution
709 of plant debris arising from biogenic sources has been much weaker during the second
710 campaign at CB and Vif, compared to three years earlier, thus showing little to no correlation
711 with characteristic biogenic tracers. This may be the reason for the weakened seasonality at
712 both CB and Vif. Secondly, the increased correlation with Ca²⁺ during 20/21 implies a better
713 correlation between plant debris and mineral dust abundance. This in turn could suggest a slight
714 increase in the strength of plant matter resuspension during the second campaign, compared to
715 2018-19.



716 **ANDRA-OPE**

717 Figure 8 shows the seasonal mean average free cellulose concentrations (ng m^{-3}) for three
718 separate sampling campaigns (2016, 2017 and 2020) at ANDRA-OPE (numerical values in
719 Table S11, SI). During the 2017 monitoring campaign, an extended period of sampling was
720 completed with samples being taken on average 5 times per week during summer. For this
721 interannual analysis, it was important to bring the number of data points in line with the datasets
722 from 2016 and 2020. Samples were removed from the 2017 dataset until the same sampling
723 frequency was obtained across all the periods (1 sample taken every sixth day). As can be seen
724 in Fig. 8, cellulose concentrations dropped significantly between 2016/2017 and 2020, with the
725 exception of the winter period. This is in a manner very similar to the variations seen at the CB
726 and Vif sampling sites from within the Grenoble metropole. The data for the winter period in

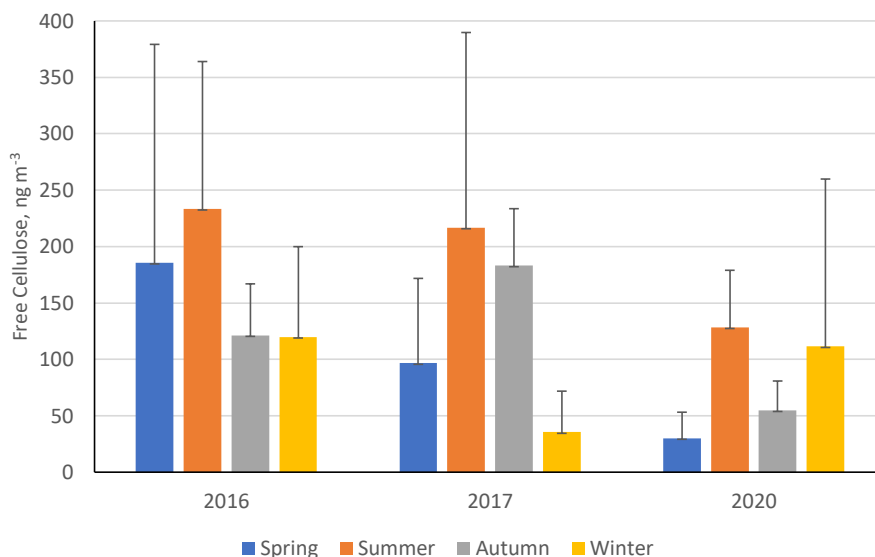


Figure 8: Seasonal mean averages of cellulose concentrations (ng m^{-3}) at ANDRA-OPE (rural site) during the three separate sampling periods: 2016, 2017 and 2020. Black error bars represent one standard deviation of the seasonal means. Only positive error bars are shown to aid clarity. Seasons are defined as: Dec-Feb (winter), Mar-May (spring), Jun-Aug (summer), Sep-Nov (autumn).

727 2020 comes predominantly from before the COVID-19 pandemic, so it is possible for the
728 significant reduction in anthropogenic activities being a major factor in the reduction of
729 atmospheric cellulose concentrations. However, it should be mentioned that agricultural



730 activities (fertilisation, harvest, ploughing, etc...) were not affected by the COVID-19
731 associated restrictions.
732 Further, we once again see a noticeable reduction in the contribution of cellulose-C to OC (%)
733 during the 2020 sampling period, compared to the two previous campaigns, especially during
734 summer and autumn (Fig. 9, numerical values Table S12, SI). This suggests that the source of
735 atmospheric plant debris became significantly weaker during 2020, when placed in the context
736 of overall OC atmospheric emission. Unlike the Grenoble metropole dataset, at ANDRA-OPE
737 the seasonal variations of cellulose concentrations and the respective contributions of cellulose-
738 C to overall OC are different. This may suggest that other emission sources of OC have varied
739 at ANDRA-OPE, compared to the more consistent OC emission within Grenoble across its
740 sampling periods.

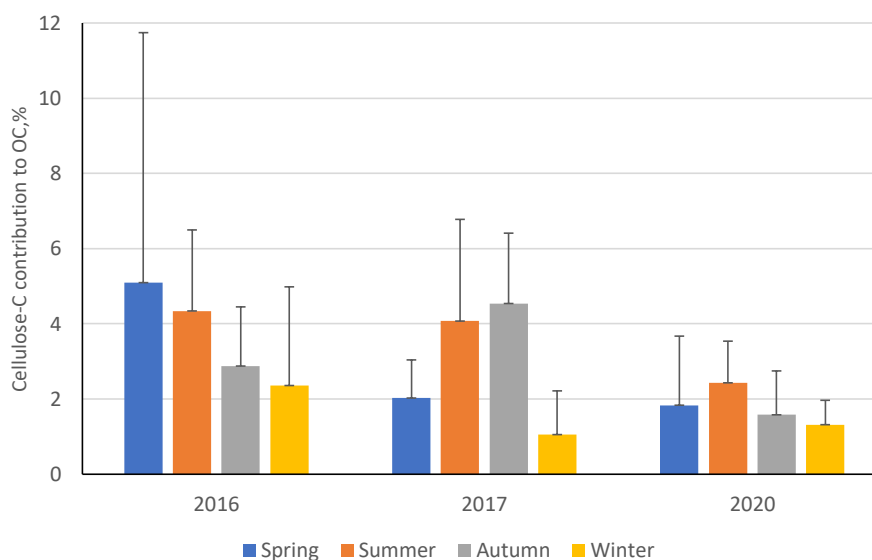


Figure 9: Percentage contribution of cellulose-carbon towards overall organic carbon (cellulose-C to OC) at ANDRA-OPE during the three separate sampling periods: 2016, 2017 and 2020. Black error bars represent one standard deviation of the seasonal means. Only positive error bars are shown to aid clarity. Seasons are defined as: Dec-Feb (winter), Mar-May (spring), Jun-Aug (summer), Sep-Nov (autumn).

741 Following these significant interannual variations within cellulose concentrations and
742 cellulose-C to OC, correlations of cellulose with source-specific tracers were completed to see
743 how the source of atmospheric plant debris has changes between the three sampling periods
744 (Table 8, p values in Table S13, SI). The three sampling periods at ANDRA-OPE exhibit
745 significant variations in their cellulose-tracer correlations. Notably, the correlations of
746 cellulose with biogenic tracers (polyols and glucose) remain generally moderate throughout,



747 and in fact are weakest during the 2016 campaign. This suggests that, at the rural site of
748 ANDRA-OPE, the significant reduction in atmospheric cellulose concentrations during 2020
749 is consistent with that of the changes within other biogenic chemical tracers. Further, during
750 the 2020 campaign, a relatively strong correlation is seen between cellulose and Ca^{2+} , a mineral
751 dust tracer, that is absent during the previous two campaigns. This potentially implies a
752 significant contribution to cellulose concentrations from an anthropogenic source, or reflects a
753 correlation to wind speed. An anthropogenic source would be unlikely however, given the rural
754 nature of this sampling site and its lack of proximity to anthropogenic inputs, outside of
755 agriculture.

Table 8: Spearman correlations (R_s) between cellulose and characteristic chemical tracers at ANDRA-OPE, across the three separate sampling periods: 2016, 2017 and 2020. A red cell indicates a positive correlation between cellulose and the selected chemical tracer, whilst a blue cell indicates a negative correlation. A colour-coded key of corresponding R_s values is to the right of the table. Note: polyols = sum of arabitol, mannitol and sorbitol.

R_s	ANDRA-OPE			
	2016	2017	2020	
Polyols	0.44	0.52	0.63	1.00
Glucose	0.21	0.57	0.41	0.66
Levoglucozan	-0.31	-0.30	-0.68	0.33
EC	-0.12	0.03	0.08	0.00
Ca^{2+}	0.23	0.11	0.62	-0.33
				-0.66
				-1.00

756 Overall, these results at ANDRA-OPE and within the Grenoble conurbation indicate for the
757 first time a large interannual variability in the sources and drivers of atmospheric cellulose, and
758 highlight our emerging knowledge of these processes.

759

760 4. Conclusions

761

762 Previous work has acknowledged the potential contribution of atmospheric cellulose to PM_{10}
763 and atmospheric OC (Bozetti et al., 2013; Borlaza et al., 2021; Yttri et al., 2011b). Yet, long-
764 term studies using cellulose as a chemical tracer for atmospheric plant debris are still rare, and
765 typically cover only few ambient conditions (Yttri et al., 2011a; Sánchez-Ochoa et al., 2007;
766 Caseiro, 2008; Yttri et al., 2011b; Alves, 2017). Thus, an investigation of ambient cellulose
767 concentrations, across a wide range of locations and site types, using a novel and sensitive
768 HPLC-PAD analysis and an improved hydrolysis method was undertaken. To date, with more



769 than 1500 samples analysed in the exact same way, this is one of the most in-depth study of
770 atmospheric cellulose, its seasonality, spatiotemporal variability and its sources.

771

772 Annual mean free cellulose concentrations were found to range between $29 \pm 38 \text{ ng m}^{-3}$ at
773 Basel to $284 \pm 225 \text{ ng m}^{-3}$ at Payerne (suburban and rural sites, respectively). All rural sites and
774 half of the urban sites showed cellulose concentrations that were highest during summer and
775 autumn, coinciding with typically higher seasonal temperatures. This seasonality differs from
776 the spring-summer maximum illustrated by Sánchez-Ochoa et al. (2007). The remaining urban
777 sites deviated significantly from this pattern, showing no evidence of seasonal cellulose
778 variations. This suggests that different sources or processes may shadow the cellulose
779 seasonality in some urban areas. Cellulose concentrations generally correlated poorly between
780 sites, which implies a source of atmospheric plant debris that is highly localised.

781

782 For the first time, correlations of cellulose with chemical tracers, that are characteristic of
783 specific emissions sources, were completed to best apportion the origins of atmospheric plant
784 debris. It was shown that plant debris arises predominantly via direct biogenic emissions,
785 particularly at rural locations. Further, the sites showing the strongest correlations with
786 biogenic tracers were the same sites that exhibited the general summer-autumn cellulose
787 maxima. A potential secondary influence towards ambient cellulose concentrations comes via
788 resuspension of previously settled plant matter, comparable to that of mineral dust. The
789 mechanism associated with this source is unknown but is unlikely to possess a traffic signature
790 at the sites investigated, given the poor cellulose correlations with EC, a known tracer for
791 anthropogenic combustion mainly related to traffic in urban areas. This may be the factor that
792 masks seasonality at some urban sites. At rural locations, agricultural activities can be a
793 significant source of cellulose into the atmosphere during harvest, as demonstrated by Samaké
794 et al. (2019b). Lastly, biomass burning is not a source of atmospheric cellulose for the sites
795 investigated here.

796

797 The annual contribution of free cellulose-derived carbon to total organic carbon ranged
798 between 0.7 and 5.9 % for the measured locations, with rural sites typically showing higher
799 contributions. It should be noted that the percentage contribution of total cellulose-derived
800 carbon to OC would be greater than the above values. While the annual mean contributions to
801 OC seem moderate, this percentage can greatly increase during episodic cellulose
802 concentration spikes. The maximum percentage contributions seen of cellulose-C to OC at



803 Payerne and ANDRA-OPE were 19.7 and 18.3% respectively, which are consistent with other
804 background sites results found in the literature. These significant episodic contributions show
805 that cellulose and plant debris can play a significant role in the atmospheric composition.

806

807 The interannual variations of the cellulose concentrations at the same locations within the
808 Grenoble metropole were then assessed. Interestingly, the cellulose concentrations and the
809 contribution (%) of cellulose-C to OC showed significant fluctuations across the two periods
810 considered. The correlations of cellulose with other chemical tracers also vary significantly.
811 Reasons behind these dramatic fluctuations are not fully understood and this highlights our
812 limited knowledge of these atmospheric processes. Reduced human activities due to the
813 COVID-19 pandemic may be a factor. Further interannual studies must be undertaken to see if
814 these variations are a common occurrence, or unique to this dataset.

815

816 Given the local-scale source of atmospheric plant debris, more monitoring campaigns similar
817 to the one in the Grenoble metropole should be performed. An increase in sampling sites
818 number, with varying micro-climatic and PM emission source characteristics, within a given
819 area should lead to a more concrete understanding of the spatial variability of plant debris. It
820 would open the road for the inclusion of cellulose into chemical transport models, in order to
821 better represent this component of the organic matter in PM, particularly important in rural
822 areas.

823

824 **Data availability:** All relevant data for this paper are archived at the IGE (Institut des
825 Géosciences de l'Environnement), and are available upon request from the corresponding
826 authors (Adam Brighty or Jean-Luc Jaffrezo).

827

828 **Acknowledgements:** The authors acknowledge the work of the many engineers in the lab at
829 IGE for the analyses (C. Voiron, R. Elazzouzi, B. Morisset, C. Le Bigaignon, J. Chazelle, A.
830 Vella, G. Fonkoh) as well as the dedicated efforts of many people at the sampling sites for
831 collecting the samples. A. M. Brighty would also like to thank S. Weber for his help and
832 guidance throughout the project. Samples from the 3 Grenoble sites were collected and
833 analysed within the program QAMECS (ADEME 1662C0029), coupled with funding from the
834 CARA program from LCSQA for the “Les Frênes” site.

835

836 **Author contributions:** JLJ was the supervisor for the Masters of AMB. He directed all the
837 personnel who performed the analysis at IGE and designed the study. VJ designed the protocol
838 for cellulose analyses. AMB performed all cellulose analyses, processed the data and wrote up
839 the manuscript. JLJ and GU were the coordinators of the atmospheric part of the Mobil’Air
840 program in Grenoble; LJB was the curator of the atmospheric Mobil’Air data. SB is the



841 coordinator of the ANDRA-OPE site and atmospheric program, and provided the samples from
842 this site. CH is the head of the NABEL network in Switzerland, provided all samples from this
843 country and directed the program for this yearly sampling; SKG was the curator of the swiss
844 data. OF is responsible for the CARA program from the LCSQA in France, and provided partial
845 funding for sample analysis at LF site. CT was responsible for the sampling by Atmo-AURA
846 at the 3 sites in the Grenoble area. All authors reviewed and commented on the manuscript.

847 **Competing interests:** The authors declare that they have no conflict of interest.

848 **References**

849 Alfarrá, M. R., Prevot, A. S. H., Szidat, S., Sandradewi, J., Weimer, S., Lanz, V. A., Schreiber,
850 D., Mohr, M., and Baltensperger, U.: Identification of the mass spectral signature of organic
851 aerosols from wood burning emissions, *Environ. Sci. Technol.*, 41, 5770–5777, 2007.

852 Alleman, L. Y., Lamaison, L., Perdrix, E., Robache, A. and Galloo, J.-C.: PM10 metal
853 concentrations and source identification using positive matrix factorization and wind sectoring
854 in a French industrial zone, *Atmospheric Research*, 96(4), 612–625,
855 <https://doi.org/10.1016/j.atmosres.2010.02.008>, 2010.

856
857 Alves, C. A.: A short review on atmospheric cellulose, *Air Qual. Atmos. Health*, 10, 669–678,
858 2017.

859 Atmo AURA: <https://www.atmo-auvergnerhonealpes.fr/>, last access: 12 April 2021.

860 Aymoz, G., Jaffrezo, J. L., Chapuis, D., Cozic, J., and Maenhaut, W.: Seasonal variation of PM
861 10 main constituents in two valleys of the French Alps. I: EC/OC fractions, *Atmos. Chem.
862 Phys.*, 7(3), 661–675, 2007.

863 Bauer, H., Claeys, M., Vermeylen, R., Schueller, E., Weinke, G., Berger, A., and Puxbaum,
864 H.: Arabitol and mannitol as tracers for the quantification of airborne fungal spores, *Atmos.
865 Environ.*, 42(3), 588–593, 2008a.

866 Birch, M. E. and Cary, R. A.: Elemental carbon-based method for monitoring occupational
867 exposures to particulate diesel exhaust, *Aerosol Sci. Technol.*, 25(3), 221–241, 1996.
868 Borlaza, L. J. S., Weber, S., Uzu, G., Jacob, V., Cañete, T., Micallef, S., Trébuchon, C., Slama,
869 R., Favez, O., Jaffrezo, J., L.: Disparities in particulate matter (PM10) origins and oxidative
870 potential at a city-scale (Grenoble, France) - Part I: Source apportionment at three neighbouring
871 sites, *Atmos. Chem. Phys.*, 21(7), 5415–5437, 2021a.

872 Borlaza, L. J. S., Weber, S., Jaffrezo, J. L., Houdier, S., Slama, R., Rieux, C., Albinet, A.,
873 Micallef, S., Trébuchon, C., and Uzu, G.: Disparities in PM₁₀ origins and oxidative potential at
874 a city-scale (Grenoble, France) - Part II: Sources of PM₁₀ oxidative potential using multiple
875 linear regression analysis and the predictive applicability of multilayer perceptron neural
876 network analysis, *Atmos. Chem. Phys.*, 21(12), 9719–9739, <https://doi.org/10.5194/acp-21-9719-2021>, 2021b.



- 878 Borlaza, L. J. S., Weber, S., Marsal, A., Uzu, G., Jacob, V., Besombes, J. L., Conil, S., and
879 Jaffrezo, J. L.: Long-term trends of PM₁₀ sources and oxidative potential in a rural site in
880 France. Submitted to Atmos. Chem. Phys. Disc., on 18/10/2021, 2021c.
- 881 Boucher, O., Randall, D., Artaxo, P., Bretherton, C., Feingold, G., Forster, P., Kerminen, V.-
882 M., Kondo, Y., Liao, H., and Lohmann, U.: Clouds and aerosols, in Climate change 2013: the
883 physical science basis. Contribution of Working Group I to the Fifth Assessment Report of the
884 Intergovernmental Panel on Climate Change, pp. 571– 657, Cambridge University Press.,
885 2013.
- 886 Bozetti, C., Daellenbach, K. R., Heuglin, C., Fermo, P., Sciare, J., Kasper-Giebl, A., Mazar,
887 Y., Abbaszade, G., El Kazzi, M., Gonzalez, R., Shuster-Meiseles, T., Flasch, M., Wolf, R.,
888 Kreplová, A., Canonaco, F., Schnelle-Kreis, J., Slowik, J. G., Zimmermann, R., Rudich, Y.,
889 Baltensperger, U., El Haddad, I., and Prévôt, A. S. H.: Size-Resolved Identification,
890 Characterisation, and Quantification of Primary Biological Organic Aerosol at a European
891 Rural Site, Environ. Sci. Technol., 50, 3425 – 3434, 2016.
- 892 Butler, G. W., and Bailey, R. W.: Chemistry and Biochemistry of Herbage, Academic Press,
893 New York, USA, 1973.
- 894 Caseiro, A. F. F.: Composição Química do Aerossol Europeu., PhD Thesis, Universidade de
895 Aveiro, Aveiro. [online] Available from: <https://core.ac.uk/download/pdf/15560924.pdf>
896 (Accessed 27 October 2020), 2008.
- 897 Cavalli, F., Viana, M., Yttri, K. E., Genberg, J., and Putaud, J.-P.: Toward a standardised
898 thermal-optical protocol for measuring atmospheric organic and elemental carbon: the
899 EUSAAR protocol, Atmos. Meas. Tech., 3(1), 79–89, 2010.
- 900 Charron, A., Polo-Rehn, L., Besombes, J. L., Golly, B., Buisson, C., Chanut, H., Marchand,
901 N., Guillaud, G., and Jaffrezo, J. L.: Identification and quantification of particulate tracers of
902 exhaust and non-exhaust vehicle emissions for source apportionment studies, Atmos. Chem.
903 Phys., 19(7), 5187–5207, <https://doi.org/10.5194/acp-19-5187-2019>, 2019.
- 904 Chevrier, F.: Chauffage au bois et qualité de l'air en Vallée de l'Arve : définition d'un système
905 de surveillance et impact d'une politique de rénovation du parc des appareils anciens., PhD
906 Thesis, Université Grenoble Alpes, Grenoble. [online] Available from: [https://tel.archives-
907 ouvertes.fr/tel-01527559](https://tel.archives-ouvertes.fr/tel-01527559) (Accessed 5 January 2021), 2016.
- 908 Denier van der Gon, H., Jozwicka, M., Hendriks, E., Gondwe, M., and Schaap, M.: Mineral
909 Dust as a component of Particulate Matters, BOP Reports, The Netherlands, 2010.
- 910 Després, V. R., Alex Huffman, J., Burrows, S. M., Hoose, C., Safatov, A. S., Buryak, G.,
911 Fröhlich-Nowoisky, J., Elbert, W., Andreae, M. O., Pöschl, U., and Jaenicke, R.: Primary
912 biological aerosol particles in the atmosphere: a review, Tellus B: Chemical and Physical
913 Meteorology, 64, 15598, 2012.
- 914 Franke, V., Zieger, P., Wideqvist, U., Acosta Navarro, J. C., Leck, C., Tunved, P., Rosati, B.,
915 Gysel, M., Salter, M. E., and Ström, J.: Chemical composition and source analysis of



- 916 carbonaceous aerosol particles at a mountaintop site in central Sweden, *Tellus B Chem. Phys.*
917 *Meteorol.*, 69(1), 1353387, <https://doi.org/10.1080/16000889.2017.1353387>, 2017.
- 918 Fuzzi, S., Andreae, M. O., Huebert, B. J., Kulmala, M., Bond, T. C., Boy, M., Doherty, S. J.,
919 Guenther, A., Kanakidou, M., and Kawamura, K.: Critical assessment of the current state of
920 scientific knowledge, terminology, and research needs concerning the role of organic aerosols
921 in the atmosphere, climate, and global change, *Atmos. Chem. Phys.*, 6(7), 2017–2038, 2006.
- 922 Gelencsér, A., May, B., Simpson, D., Sánchez-Ochoa, A., Kasper-Giebl, A., Puxbaum, H.,
923 Caseiro, A., Pio, C. and Legrand, M.: Source apportionment of PM_{2.5} organic aerosol over
924 Europe: Primary/secondary, natural/anthropogenic, and fossil/biogenic origin, *J. Geophys.*
925 *Res.*, 112(D23), D23S04, <https://doi.org/10.1029/2006JD008094>, 2007.
- 926 Gelencsér, A.: *Carbonaceous Aerosol*, 1st edn, Springer, The Netherlands, 350 pages, 2004.
- 927 Giannoni, M., Martellini, T., Del Bubba, M., Gambaro, A., Zangrando, R., Chiari, M., Lepri,
928 L., and Cincinelli, A.: The use of levoglucosan for tracing biomass burning in PM_{2.5} samples in
929 Tuscany (Italy), *Environmental Pollution*, 167, 7–15, 2012.
- 930 Golly, B., Waked, A., Weber, S., Samaké, A., Jacob, V., Conil, S., Rangonio, J., Chrétien, E.,
931 Vagnot, M. P., Robic, P. Y., Besombes, J. L., and Jaffrezo, J. L.: Organic Markers And OC
932 Source Apportionment For Seasonal Variations Of PM_{2.5} At 5 Rural Sites In France, *Atmos.*
933 *Environ.*, 198, 142–157, <https://doi.org/10.1016/J.Atmosenv.2018.10.027>, 2019.
- 934 Graham, B., Guyon, P., Taylor, P. E., Artaxo, P., Maenhaut, W., Glovsky, M. M., Flagan, R.
935 C., and Andreae, M. O.: Organic compounds present in the natural Amazonian aerosol:
936 Characterization by gas chromatography-mass spectrometry: Organic compounds in
937 Amazonian aerosols., *J. Geophys. Res. Atmospheres*, 108(D24), 4766, 2003.
- 938 Grange, S. K., Fischer, A., Zellweger, C., Alastuey, A., Querol, X., Jaffrezo, J. L., Uzu, G.,
939 and Hueglin, C.: Switzerland's PM₁₀ and PM_{2.5} environmental increments show the
940 importance of non-exhaust emissions, *Atmos. Environ.*, submitted (on 22/06/21).
- 941 Jaenicke, R.: Abundance of cellular material and proteins in the atmosphere, *Science*,
942 308(5718), 73–73, <https://doi.org/10.1126/science.1106335>, 2005.
- 943 Jaffrezo, J. L., Calas, N., and Bouchet, M.: Carboxylic acids measurements with ionic
944 chromatography, *Atmos. Environ.*, 32(14), 2705–2708, 1998.
- 945 Jia, Y., Bhat, S., and Fraser, M. P.: Characterization of saccharides and other organic
946 compounds in fine particles and the use of saccharides to track primary biologically derived
947 carbon sources, *Atmos. Environ.*, 44(5), 724–732, 2010a.
- 948 Karagulian, F., Belis, C. A., Dora, C. F. C., Prüss-Ustün, A. M., Bonjour, S., Adair-Rohani,
949 and H., Amann, M.: Contributions to cities' ambient particulate matter (PM): A systematic
950 review of local source contributions at global level, *Atmos. Environ.*, 120, 475–483, 2015.
- 951 Klimont, Z., Kupiainen, K., Heyes, C., Purohit, P., Cofala, J., Rafaj, P., Borken-Kleefeld, J.,
952 and Schöpp, W.: Global anthropogenic emissions of particulate matter including black carbon,
953 *Atmos. Chem. Phys.*, 17, 8681–8723, 2017.



- 954 Kunit, M., and Puxbaum, H.: Enzymatic determination of the cellulose content of atmospheric
955 aerosols, *Atmos. Environ.*, 30, 1233–1236, 1996.
- 956 Liang, L., Engling, G., Du, Z., Cheng, Y., Duan, F., Liu, X., and He, K.: Seasonal variations
957 and source estimation of saccharides in atmospheric particulate matter in Beijing, China,
958 *Chemosphere*, 150, 365–377, 2016.
- 959 Madsen, D., Azeem, H. A., Sandahl, M., van Hees, P., and Husted, B.: Levoglucosan as a
960 Tracer for Smouldering Fire, *Fire Technology*, 54, 1871–1885, 2018.
- 961 Martin, S. T., Andreae, O. M., Artaxo, P., Baumgardner, D., Chen, Q., Goldenstein, A. H.,
962 Guenther, A., Heald, C. L., Mayol-Bracero, O. L., McMurry, P. H., Pauliquevis, T., Pöschl,
963 U., Prather, K. A., Roberts, G. C., Saleska, S. R., Silva Dias, M. A., Spracklen, D. V.,
964 Swietlicki, E., and Trebs, I.: Sources and properties of Amazonian aerosol particles, *Rev.
965 Geophys*, 48(2), <https://doi.org/10.1029/2008RG000280>, 2010.
- 966 Martínez, A., Larrañaga, A., Pérez, J., Descals, E., and Pozo, J.: Temperature affects leaf litter
967 decomposition in low-order forest streams: field and microcosm approaches, *FEMS Microb.
968 Ecol.*, 87, 257–267, 2014.
- 969 Medeiros, P. M., Conte, M. H., Weber, J. C., and Simoneit, B. R. T.: Sugars as source indicators
970 of biogenic organic carbon in aerosols collected above the Howland Experimental Forest,
971 Maine, *Atmos. Environ.*, 40(9), 1694–1705, 2006.
- 972 Michoud, V., Hallemans, E., Chiappini, L., Leoz-Garziandia, E., Colomb, A., Dusanter, S.,
973 Fronval, I., Gheusi, F., Jaffrezo, J. L., Léonardis, T., Locoge, N., Marchand, N., Sauvage, S.,
974 Sciare, J., and Doussin, J. F.: Molecular characterization of gaseous and particulate oxygenated
975 compounds at a remote site in Cape Corsica in the western Mediterranean basin, *Atmos. Chem.
976 Phys.*, 21(10), 8067–8088, <https://doi.org/10.5194/acp-21-8067-2021>, 2021.
- 977 Mobil’Air QAMECS Program: [https://mobilair.univ-grenoble-alpes.fr/mobilair/projets-
978 associés/projets-associés-743738.htm?RH=2206232030103086](https://mobilair.univ-grenoble-alpes.fr/mobilair/projets-associés/projets-associés-743738.htm?RH=2206232030103086), last access: 13 April 2021.
- 979 Nozière, B., Kalberer, M., Claeys, M., Allan, J., D’Anna, B., Decesari, S., Finessi, E., Glasius,
980 M., Grgić, I., Hamilton, J. F., Hoffmann, T., Iinuma, Y., Jaoui, M., Kahnt, A., Kampf, C. J.,
981 Kourtchev, I., Maenhaut, W., Marsden, N., Saarikoski, S., Schnelle-Kreis, J., Surratt, J. D.,
982 Szidat, S., Szmigielski, R., and Wisthaler, A.: The molecular identification of organic
983 compounds in the atmosphere: state of the art and challenges, *Chem. Rev.*, 115(10), 3919–
984 3983, <https://doi.org/10.1021/cr5003485>, 2015.
- 985 OPE-ANDRA Atmospheric Station: <http://ope.andra.fr/index.php?lang=fr>, last access: 6
986 January 2021.
- 987 Peccia, J., Hospodsky, D., and Bibby, K.: New Directions : A revolution in DNA sequencing
988 now allows for the meaningful integration of biology with aerosol science, *Atmos. Environ.*,
989 45, 1896–1897, 2011.
- 990 Penner, J. E., Andreae, M., Annegarn, H., Barrie, L., Feichter, J., Hegg, D., Jayaraman, A.,
991 Leaitch, R., Murphy, D., Nganga, J., and Pitari, G.: *Aerosols, their Direct and Indirect Effects*,
992 *Climate Change 2001: The Scientific Basis.*, Cambridge University Press, Cambridge, 2001.



- 993 Pöschl, U., Martin, S. T., Sinha, B., Chen, Q., Gunthe, S. S., Huffman, J. A., Borrmann, S.,
994 Farmer, D. K., Garland, R. M., Helas, G., Jimenez, J. L., King, S. M., Manzi, A., Mikhailov,
995 E., Pauliquevis, T., Petters, M. D., Prenni, A. J., Roldin, P., Rose, D., Schneider, J., Su, H.,
996 Zorn, S. R., Artaxo, P., and Andreae, M. O.: Rainforest Aerosols as Biogenic Nuclei of Clouds
997 and Precipitation in the Amazon, *Science*, 329 (5998), 1513–1516, 2010.
- 998 Pöschl, U.: Atmospheric Aerosols: Composition, Transformation, Climate and Health Effects,
999 *Angew. Chem. Int. Ed.*, 44(46), 7520 – 7540, 2005.
- 1000 Putaud, J.-P., Raes, F., Van Dingenen, R., Brüggemann, E., Facchini, M.-C., Decesari, S.,
1001 Fuzzi, S., Gehrig, R., Hüglin, C., Laj, P., Lorbeer, G., Maenhaut, W., Mihalopoulos, N., Müller,
1002 K., Querol, X., Rodriguez, S., Schneider, J., Spindler, G., Brink, H. ten, Tørseth, K., and
1003 Wiedensohler, A.: A European aerosol phenomenology 2: chemical characteristics of
1004 particulate matter at kerbside, urban, rural and background sites in Europe, *Atmos. Environ.*,
1005 38(16), 2579–2595, 2004a.
- 1006 Putaud, J.-P., Van Dingenen, R., Alastuey, A., Bauer, H., Birmili, W., Cyrus, J., Flentje, H.,
1007 Fuzzi, S., Gehrig, R., Hansson, H. C., Harrison, R. M., Herrmann, H., Hitzenberger, R., Hüglin,
1008 C., Jones, A. M., Kasper-Giebl, A., Kiss, G., Kousa, A., Kuhlbusch, T. A. J., Löschau, G.,
1009 Maenhaut, W., Molnar, A., Moreno, T., Pekkanen, J., Perrino, C., Pitz, M., Puxbaum, H.,
1010 Querol, X., Rodriguez, S., Salma, I., Schwarz, J., Smolik, J., Schneider, J., Spindler, G., ten
1011 Brink, H., Tursic, J., Viana, M., Wiedensohler, A. and Raes, F.: A European aerosol
1012 phenomenology – 3: Physical and chemical characteristics of particulate matter from 60 rural,
1013 urban, and kerbside sites across Europe, *Atmos. Environ.*, 44(10), 1308–1320,
1014 <https://doi.org/10.1016/j.atmosenv.2009.12.011>, 2010.
- 1015 Puxbaum, H., and Tenze-Kunit, M.: Size distribution and seasonal variation of atmospheric
1016 cellulose, *Atmos. Environ.*, 37(26), 3693–3699, 2003.
- 1017 Rosenfeld, D., Lohmann, U., Raga, G. B., O’Dowd, C. D., Kulmala, M., Fuzzi, S., Reissell,
1018 A., and Andreae, M. O.: Flood or Drought: How Do Aerosols Affect Precipitation?, *Science*,
1019 321(5894), 1309–1313, 2008.
- 1020 Samaké, A., Jaffrezo, J.-L., Favez, O., Weber, S., Jacob, V., Albinet, A., Riffault, V., Perdrix,
1021 E., Waked, A., Golly, B., Salameh, D., Chevrier, F., Oliveira, D. M., Bonnaire, N., Besombes,
1022 J.-L., Martins, J. M. F., Conil, S., Guillaud, G., Mesbah, B., Rocq, B., Robic, P.-Y., Hulin, A.,
1023 Le Meur, S., Descheemaeker, M., Chretien, E., Marchand, N. and Uzu, G.: Polyols and
1024 glucose particulate species as tracers of primary biogenic organic aerosols at 28 French sites,
1025 *Atmos. Chem. Phys.*, 19(5), 3357–3374, <https://doi.org/10.5194/acp-19-3357-2019>, 2019a.
- 1026 Samaké, A., Jaffrezo, J.-L., Favez, O., Weber, S., Jacob, V., Albinet, A., Riffault, V., Perdrix, E.,
1027 Waked, A., Golly, B., Salameh, D., Chevrier, F., Oliveira, D. M., Bonnaire, N., Besombes, J.-L.,
1028 Martins, J. M. F., Conil, S., Guillaud, G., Mesbah, B., Rocq, B., Robic, P.-Y., Hulin, A., Le Meur,
1029 S., Descheemaeker, M., Chretien, E., Marchand, N. and Uzu, G.: Polyols and glucose as tracers
1030 of primary biogenic organic aerosol: influence of environmental factors on ambient air
1031 concentrations and spatial distribution over France, *Atmos. Chem. Phys.*, <https://doi.org/10.5194/acp-19-11013-2019>, 2019b.



- 1033 Samaké, A., Bonin, A., Jaffrezo, J. L., Taberlet, P., Uzu, G., Jacob, V., Conil, S., and Martins,
1034 J. M. F.: High levels of Primary Biogenic Organic Aerosols in the atmosphere in summer are
1035 driven by only a few microorganisms from the leaves of surrounding plants, *Atmos. Chem.*
1036 *Phys.*, <https://doi.org/10.5194/acp-20-5609-2020>, 2020.
- 1037 Samake, A., Martins, J. M., Bonin, A., Uzu, G., Taberlet, P., Conil, S., Favez, O., Thomasson,
1038 A., Chazeau, B., Marchand, N., and Jaffrezo, J. L.: Variability of the atmospheric PM₁₀
1039 microbiome in three climatic regions of France, *Frontiers in Microbiology*, <https://doi.org/10.3389/fmicb.2020.576750>, 2021.
- 1041 Sánchez-Ochoa, A., Kasper-Giebl, A., Puxbaum, H., Gelencsér, A., Legrand, M., and Pio, C.:
1042 Concentration of atmospheric cellulose: A proxy for plant debris across a west-east transect
1043 over Europe, *J. Geophys. Res.*, 112, <https://doi.org/10.1029/2006JD008180>, 2007.
- 1044 Schmidl, C.: PM₁₀—Quellenprofile von Holzrauchemissionen aus Kleinf Feuerungen,
1045 Diplomarbeit, Inst. für Chem. Technol. und Analytik, Tech. Univ. Wien, Vienna, 2005.
- 1046 Verma, S. K., Kawamura, K., Chen, J., and Fu, P.: Thirteen years of observations on primary
1047 sugars and sugar alcohols over remote Chichijima Island in the western North Pacific, *Atmos.*
1048 *Chem. Phys.*, 18(1), 81–101, 2018.
- 1049 Waked, A., Favez, O., Alleman, L. Y., Piot, C., Petit, J.-E., Delaunay, T., Verlinden, E., Golly,
1050 B., Besombes, J.-L., Jaffrezo, J.-L., and Leoz-Garziandia, E.: Source apportionment of PM₁₀
1051 in a north-western Europe regional urban background site (Lens, France) using positive matrix
1052 factorization and including primary biogenic emissions, *Atmos. Chem. Phys.*, 14(7), 3325–
1053 3346, 2014.
- 1054 Wagenbrenner, N. S., Chung, S. H., and Lamb, B. K.: A large source of dust missing in
1055 Particulate Matter emission inventories? Wind erosion of post-fire landscapes, *Elem. Sci.*
1056 *Anth.*, 5(2), <https://doi.org/10.1525/elementa.185>, 2017.
- 1057 Weber, S., Salameh, D., Albinet, A., Alleman, L. Y., Waked, A., Besombes, J.-L., Jacob, V.,
1058 Guillaud, G., Meshbah, B., Rocq, B., Hulin, A., Dominik-Sègue, M., Chrétien, E., Jaffrezo, J.-
1059 L. and Favez, O.: Comparison of PM₁₀ Sources Profiles at 15 French Sites Using a
1060 Harmonized Constrained Positive Matrix Factorization Approach, *Atmosphere*, 10(6), 310,
1061 <https://doi.org/10.3390/atmos10060310>, 2019.
- 1062 Winiwarter, W., Bauer, H., Caseiro, A., and Puxbaum, H.: Quantifying emissions of primary
1063 biological aerosol particle mass in Europe, *Atmos. Environ.*, 43, 1403–1409, 2009.
- 1064 Wu, C. and Yu, J. Z.: Determination of primary combustion source organic carbon-to-
1065 elemental carbon (OC/EC) ratio using ambient OC and EC measurements: secondary OC-EC
1066 correlation minimization method, *Atmos. Chem. Phys.*, 16, 5453–5465, 2016.
- 1067 Yttri, K. E., Aas, W., Bjerke, A., Cape, J. N., Cavalli, F., Ceburnis, D., Dye, C., Emblico, L.,
1068 Facchini, M. C., Forster, C., Hanssen, J. E., Hansson, H. C., Jennings, S. G., Maenhaut, W.,
1069 Putaud, J. P., and Tørseth, K.: Elemental and organic carbon in PM₁₀: a one year
1070 measurement campaign within the European Monitoring and Evaluation Programme EMEP,
1071 *Atmos. Chem. Phys.*, 7, 5711–5725, <https://doi.org/10.5194/acp-7-5711-2007>, 2007.



- 1072 Yttri, K. E., Simpson, D., Stenström, K., Puxbaum, H. and Svendby, T.: Source apportionment
1073 of the carbonaceous aerosol in Norway – quantitative estimates based on ^{14}C , thermal-optical
1074 and organic tracer analysis, *Atmos. Chem. Phys. Discuss.*, 11(3), 7375–7422, 2011a.
- 1075 Yttri, K. E., Simpson, D., Nøjgaard, J. K., Kristensen, K., Genberg, J., Stenström, K.,
1076 Swietlicki, E., Hillamo, R., Aurela, M., Bauer, H., Offenberg, J. H., Jaoui, M., Dye, C.,
1077 Eckhardt, S., Burkhardt, J. F., Stohl, A., and Glasius, M.: Source apportionment of the summer
1078 time carbonaceous aerosol at Nordic rural background sites, *Atmos. Chem. Phys.*, 11, 13339 –
1079 13357, 2011b.
- 1080 Zhang, T., Engling, G., Chan, C. Y., Zhang, Y. N., Zhang, Z. S., Lin, M., Sang, X. F., Li, Y.
1081 D., and Li, Y. S.: Contribution of fungal spores to particulate matter in a tropical rainforest,
1082 *Environ. Res. Lett.*, 5(2), 24010, 2010.
- 1083 Zhu, C., Kawamura, K., and Kunwar, B.: Organic tracers of primary biological aerosol
1084 particles at subtropical Okinawa Island in the western North Pacific Rim: Organic biomarkers
1085 in the north pacific, *J. Geophys. Res. Atmospheres*, 120(11), 5504–5523, 2015.